"Materials-Design-Interface" Programme Towards Establishment of Demo Design Criteria for In-Vessel Components (DDC-IC)

Nasr Ghoniem; Eberhard Diegele, Michael Gorley, Gerald Pintsuk, Gianfranco Federici, Sergei Dudarev, Manminda Kalsey, Fabio Cismondi

"Materials-Design-Interface" Programme towards Establishment of DEMO Design Criteria for In-Vessel Components (DDC-IC)

Nasr Ghoniem; Eberhard Diegele, Michael Gorley, Gerard Pintsuk, Gianfranco Federici, Sergei Dudarev, Manminda Kalsey, and Fabio Cismondi

Executive Summary

Design rules for mechanical components in nuclear environment are based on either global strength limits or local fracture limits. The current ITER Structural Design Criteria (SDC) for In Vessel Components (SDC-IC) are based on extensions of the AFCEN – RCC-MR [today RCC-MRx] and ASME code – Section III Division 4. We briefly discuss the current status of the blanket and divertor options of the EUROfusion DEMO program, followed by a description of the materials database and associated design limits. We address inadequancies in these design rules, and show that modifications and extensions are necessary for the design of Demonstration Power Plant components (DEMO). We then present a potential path forward towards a more precise design-by-analysis approach and a strategy for the development of DEMO Design Criteria. This is based on a top-down approach, where three levels of analysis are performed.

In level I (continuum-elastic) , an enhanced elastic analysis is required, where multi-physics simulations are perfomed to couple heat transfer, fluid flow and elastic structual analysis, in an effort to optimize the design and select amongst competing concepts. Although the structural part of the analysis is elastic, it is enhanced by: (a) augmentling the elastic limits to allow for work-hardening capablities (e.g. limits on plastic collapse, ductility exhausion, and Neuber methods close to notches, etc.), and (b) through simplified Bree-type of analysis for ratcheting.

In the second level of analysis (continuum-elastic-plastic), a critical zone is isloated with its approapriate boundary conditions from level-I, and a detailed continuum elasto-plastic (and/or elasto-viscoplastic) analysis is performed to improve the predictions of the elastic analysis alone. Experimental validation will be required, especially for cyclic plasticity (creep, fatigue, and creep-fatigue). Fracture analysis is performed with the J-integral, including the effects of plasticity. The effects of environmental degradation (irradiation, corrosion, erosion) can be taken into account during implementation of this analysis via: (a) changes in material properties, geometry, and design limits; and (b) inclusion of inelastic radiation strains (e.g. swelling, and irradiation creep).

In the third level of analysis (continuum, microstructure-based, elasto-viscoplastic) a smaller Representative Volume Element (RVE) is selected with its appropriate boundary

conditions and subdivided into individual grains with texture. A dislocation-based crystal plasticity model is to be coupled with a Cohesive Zone Model (CZM) of fracture, or with a distributed damage model. Several realizations of the geometry may be necessary for predcitions. The constitutive relations in level-III analysis are to be derived from a combination of: (a) experimental data if available (especially for unirradiated materials), (b) lower length-scale material models (especially for irradiated and/or environmentally-affected materials). Such lower length-scale models themselves at the meso-scale (Dislocation Dynamics) can provide data on dislocation glide/climb motion, interaction with irradiation-induced obstacles, and reaction rates to level-III models. At the smallest length scales, atomistic models (Molecular Dynamics and Kinetic Monte Carlo) can be used to generate necessary data for mesosclae simulations.

With this type of Multiscale Design Procedure, the design of a fusion component can be realized at increasing levels of certainty without excessive conservatism. The methodology provides an iterative process as the methods mature and feedback loops are established between these three levels of analsyis on the one hand, and the science-approach represented by discrete defect dynamics (mesoscale) and atomistic simulations on the other.

TABLE OF CONTENTS

1. Introduction & the Need for DDC-IC Design Guidelines

The anticipated operating environment of components in a fusion power plant involves extreme conditions of heat flux, plasma particle flux and radiation fields (*e.g.* high-energy neutrons) as well as magnetic fields. Hydrogen, including radioactive tritium, will permeate all structures. Loading conditions may include strong transients under both normal and off-normal conditions, as well as warm and cold shut down for maintenance. Survival within this environment will be challenging.

But survival of in-vessel components alone is not sufficient. They must satisfy a set of requirements to fulfill their own functions as well as overall plant requirements. For example, they must operate at elevated temperatures to generate electricity. They must not contain elements that would lead to unacceptable safety risks or waste disposal burdens. Because failures can have catastrophic consequences on plant operations, and overall plant availability must be high, extremely high confidence in the reliability of components is needed. Following the strategy as in ITER: The vacuum vessel is identified as barrier to ensure public safety, nevertheless, very high requirements on safety and reliability are put on in-vessel components as of "protection of investment".
Requirements for a practical and attractive energy source are well known, following many years of integrated conceptual design studies. What is not known is whether any of our existing design concepts can meet these requirements. If we cannot establish acceptable solutions, then fusion will never fulfill its promise as a source of energy for mankind.

Since the early days of fusion research, it was clear that new materials would be needed to survive the fusion environment and meet the operating and safety requirements. Large materials research programs have been carried out worldwide, leading to the identification and characterization of a small number of candidate structural materials. Even after many years of research and development, there are still gaps in our knowledge of materials behavior (especially under neutron irradiation) and uncertainties remain in the choice of materials for certain components (such as divertors). However, research on individual material properties, informed by conceptual design studies, is not sufficient to answer the fundamental questions of survivability and performance of in-vessel components, which is absolutely required for fusion to be useful as an energy source. The mechanical behavior of components in the fusion environment is highly complex and highly design dependent, requiring research into critical design-dependent phenomena that might lead to failure. This we call the "materials-design interface".

Properties are almost always strongly dependent on the history of temperature and stress in the component. These are adjustable parameters. Solutions often can be found if basic materials properties are used to determine mechanical behavior, which then can be used to modify designs to alleviate problems. Success depends upon tight coupling of materials properties, mechanical behavior and component design.

Such efforts on the mechanical behavior of components have been performed within the ITER project. ITER has advanced the state-of-the-art in methods for fusion component "design by analysis", design rules and component validation. However, the requirements, designs and materials for ITER are all very different from those of a fusion power plant. ITER has no breeding requirement (which impacts design choices and design details), operates at low temperature and will experience very low neutron dose. The materials chosen for ITER could not be used in a power plant. We urgently need to extend the initial work within EUROfusion and initiate a similar level of activity specific to the designs and materials we expect will be used in DEMO.

The main objective of this report is to outline a new design methodology that is based on embodiments of multi-physics and multiscale simulations in a coherent way. This requires strong integration between the design community and the materials science community to continually reduce design uncertainties on the one hand, and to focus multiscale modeling efforts on the other. We discuss briefly the current Breeding Blanket (BB) and Divertor (DIV) options of the DEMO project in the next section. This is followed by a presentation of the current state of the materials data base and ITER design rules in section 3. Reasons behind the need for updated design rules and the inadequacy of current ITER design procedures are given in section 4. A review of the DEMO Design Criteria (DDC) is then given in section 5. The following section 6 covers a suggested design procedure that combines Multiphysics with Hierarchical Multiscale Design methodology (HMDM). Deployment timelines and resources are discussed in section 7, and finally conclusions and recommendations are articulated in section 8.

2. EUROfusion DEMO Breeding Blanket and Divertor Design Options

2.1. Breeding Blanket design options

In the frame of the EUROfusion Consortium activities the Helium Cooled Pebble Bed (HCPB), the Helium Cooled Lithium Lead (HCLL), the Water Cooled Lithium Lead (WCLL) and the Dual Coolant Lithium Lead (DCLL) have been identified in the Roadmap (Romanelli, 2012) as candidate concepts for the EU DEMO (see Figure 1) (Boccaccini, L.V., & al., 2016) (Federici, et al., 2014). For the four concepts, the candidate structural material is EUROFER (reference is the grade 97).

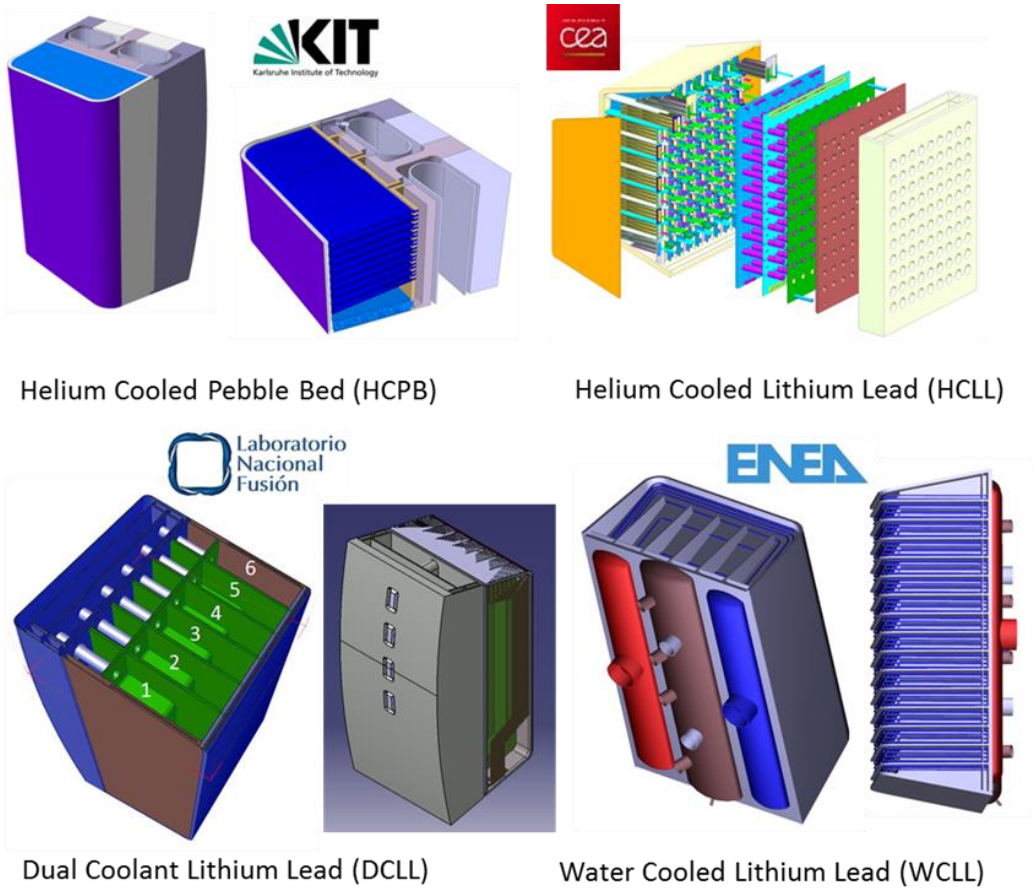

Figure 1: The 4 BB concepts studied for DEMO since 2014 in the frame of the EUROfusion activities: HCPB, HCLL, WCLL and DCLL.

The main characteristics of the considered breeder/neutron multipliers and coolants are the following.

The **solid breeder concept** (HCPB):

- Uses a Li-ceramic (Li_4SiO_4 or Li_2TiO_3) as breeder and Be/Be-alloy as neutron multiplier in form of pebble beds; with ^6Li enrichment of 50-70% it is possible to reach TBR of 1.20 already at about 50 cm of breeder thickness in the outboard segment. The concept promises very good neutronic performance.
- Some concerns for the concept are: the possible accumulation of tritium inventory in the solid material in particular in Be; the exothermic reaction of Be with steam (in case of First Wall cooled by water) above 600°C with H production (very critical issues in case of water as coolant). Attention should be paid to the tritium permeation from the breeder zone to the coolant.

The **liquid breeder concepts** (HCLL, WCLL and DCLL):

- Use a PbLi alloy at eutectic conditions at a melting temperature of about 235°C. ^6Li enrichments of about 90% lead to TBR of 1.20 obtained with breeder thickness of about 70 cm in the outboard segment. Tritium extraction is realized recirculating the liquid PbLi outside the VV in dedicated closed loops. The advantages of PbLi lie in the possibility of continuous replenishment of the 6Li and in the good thermal properties that make the cooling of internal structures easier.
- Drawbacks are in the PbLi activation, in the chemical activity with water, and in corrosion with steel structures. Tritium has very low solubility in PbLi and therefore there is a high tendency of tritium permeation (into the coolant or through the pipes). To reduce corrosion issues or tritium permeation, barriers (like Aluminum-based) on the steel at the PbLi side are proposed. The PbLi circuits have to be designed to allow degassing of He that is formed in PbLi under irradiation during operation. Furthermore, the PbLi circuits have to be designed to allow a most complete drainage (to reduce the weight of the segment during RM).

The **water** as a coolant (WCLL):

- Offers high heat transfer performances, requiring low pumping power and its cooling technology is well developed. For electricity production, the typical Pressurized Water Reactor (PWR) conditions have been proposed for fusion power plants (285-325°C at 15.5 MPa) with thermal efficiency of ~33%.
- The issues of water usage are mostly in the compatibility with the present EUROFER97: the operating temperatures are below the DBTT of steel irradiated to levels greater than 20 dpa, the corrosion should be controlled as well as its activation products. Furthermore, reaction of water with metals (e.g. W) at high temperature can produce H with detonation risks.

The **Helium** as a coolant (HCPB, HCLL and partly DCLL):

- Is compatible with almost all the materials and its temperature range can be adjusted to a wide spectrum of material conditions and needs; at high temperature it can perform at higher efficiency in the energy conversion system.
- The disadvantages of helium relate to its performance as a coolant (low heat transfer capability, necessity of large temperature differences between inlet and outlet) and on the low level of maturity of the component technology (e.g. heat exchangers, compressors). Helium transparency of neutrons requires the design of additional shielding in the blanket. In the present PPPT blanket systems a temperature range of 300-500°C at a pressure of 8 MPa has been selected for He cooling as compromise.

The main characteristics and materials of the four BBs studied in EU are summarized in the following Table 1.

Table 1: main characteristics and materials of the 4 BB studied in EU for DEMO.

	Structural material	Coolant	Breder/neutron multiplier	T extraction
HCPB	EUROFER	Helium,8MPa, 300-500°C	Li_4SiO_4 / Be	Low pressure He purge
HCLL	EUROFER	Helium, 300-500°C, 8MPa	Pb-16Li/ Pb-16Li	Extraction from recirculating PbLi
WCLL	EUROFER	Water, 15.5MPa, 285(295)-325°C	Pb-16Li/ Pb-16Li	Extraction from recirculating PbLi
DCLL	EUROFER	PbLi (300-540°C) He (300-425°C, 8 MPa)	Pb-16Li/ Pb-16Li	Extraction from recirculating PbLi

The main architecture of the HCPB, HCLL and WCLL foresees a strict division among coolant and T-breeder zone. The coolant at high pressure (water or He) cools directly the steel structure flowing mainly in small channels or tubes, whilst a T carrier (a purge gas for the solid or the breeder PbLi itself in liquid breeder concepts) fills the breeder zone and flows in independent loops at low pressure transporting T outside the reactor (see Figure 2). Also, if PbLi is used as carrier, its recirculation rate (10-20 inventories per day in WCLL and HCLL) is so slow that no significant heat is removed in these loops. The same is valid for the He purge in the HCPB.

The DCLL concept differs from this architecture. In this case, the velocity of the PbLi is an order of magnitude higher so that a significant quantity of heat can be removed by the PbLi loop (up to 50%). The remaining heat is removed by helium that flows like in HCPB and HCLL in small channels of the steel structures. To allow the PbLi flow (reducing the pressure drops for MHD interaction with the magnetic fields) electrically insulating layers separate the liquid metal from the conducting steel walls. This insulation can be realised in form of a so

called Flow Channel Insert (FCI) made by a steel-alumina sandwich or SiC. The DCLL version used in PPPT studies operates at a lower temperature range; this means lower than 550°C so that EUROFER97 can be used as structural material in the blanket and the external loops can use conventional materials (in contrast to the US version which is designed to operate with max outlet temperatures of PbLi up to 700°C with the necessity to develop high temperature materials and effective protection vs. corrosion).

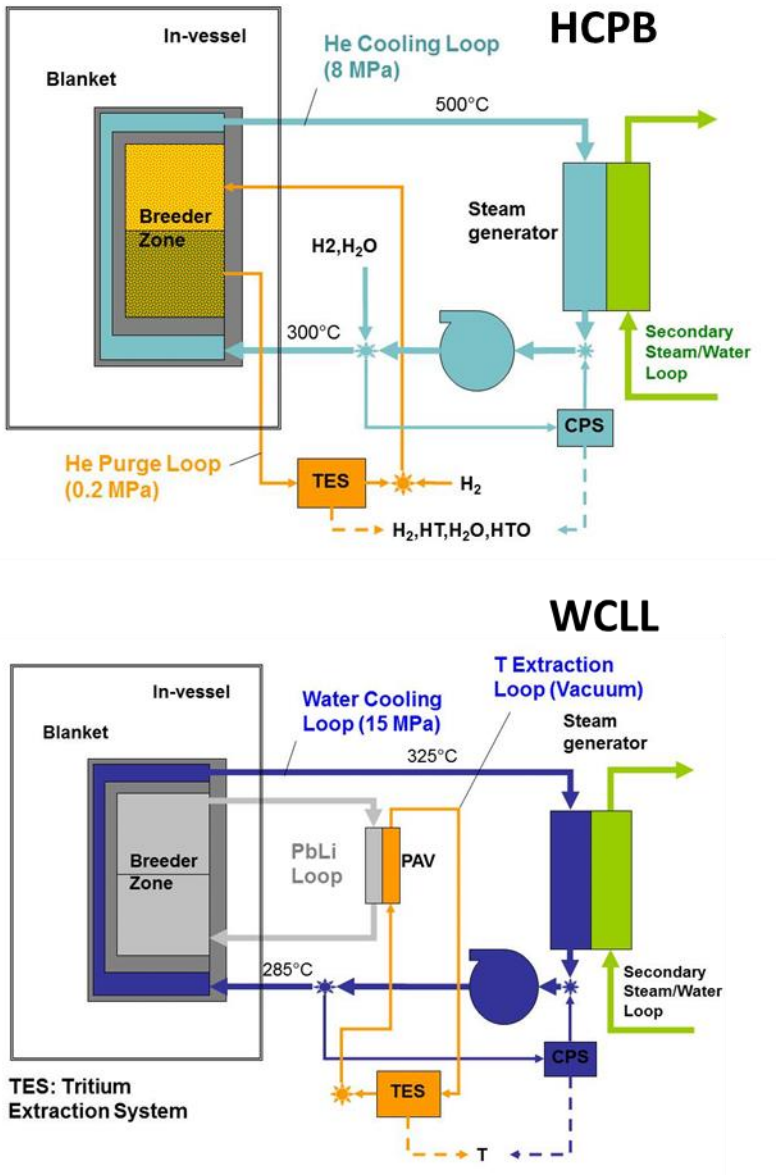

Figure 2: Schematic view of the common architecture adopted by HCPB, HCLL and WCLL

The manufacturing technologies are a key aspect to be considered in the design process of blanket components. Several studies done on typical DEMO blanket and TBM design have already identified typologies of sub-components and joints that should be applied for the manufacturing of the breeding blanket for the DEMO. These components include e.g. EUROFER97 plates with channels for FW or breeder cooling plates, double-wall tubes for water cooling in PbLi pools, W layers as plasma FW protection. Several manufacturing technologies have been tested and developed in the EU laboratories with industry participation, e.g. HIPing in different configuration ("laser reconstruction", "assembly of bended plates and tubes", etc.), spark erosion for long channels production, bending technology for large FW plates or thin breeder cooling plates, and also selective laser sintering technology with EUROFER powder. Laser and electron beam technology have been tested and partially qualified for the assembly of these components.

2.2. Divertor design options

Tungsten and copper-base materials are considered for the divertor plasma-facing armor and heat sink, respectively. The materials were selected as unique candidates under the consideration of plasma compatibility, activation, thermal conductivity and mechanical stability under neutron irradiation. The cooling channel has a circular cross section whereas the heat sink body is not necessarily limited to a pipe form. The minimum initial thickness of the armor (to the surface) is specified to be 5 mm assuming that this thickness would fulfill the minimum required component erosion lifetime of 2 full-power year (fpy) specified for a DEMO. The minimum allowed thickness of the cooling pipe of 1.5 mm was defined taking into account the loss of material due to the corrosion and erosion of the liner by the coolant flow at elevated temperatures (>140°C).

Water cooling is the primary option (baseline) for the entire divertor system while helium cooling is considered only as a back-up option being subject to long-term development. The temperature and pressure of water coolant in the target ranges from 130°C (inlet) to about 140°C (outlet) and from about 3.5 MPa (outlet) to 5 MPa (inlet), respectively The local peak speed of the coolant is limited to 12 m/s to mitigate impact on erosion. 20 MW/m^2 was specified as the local maximum heat flux peaking at the strike point on the target plate.

ITER-like tungsten monoblock

The baseline design concept for the EU DEMO divertor was inherited from the ITER divertor target design: a tungsten monoblock-type model consisting of a copper alloy (CuCrZr) pipe as heat sink and tungsten blocks as armor surrounding the pipe (see Figure 3). The pipe and blocks are joined via a thick copper interlayer. The dimension was significantly reduced from the original ITER design (e.g. width from 28 mm to 23 mm, monoblock thickness from 12 mm to 4 mm) in order to relax the thermal stress The inner diameter and thickness of the cooling pipe is 12 mm and 1.5 mm, respectively. The copper interlayer is 1 mm thick. As fabrication technology HRP (Hot Radial Press) technique is employed where the process was

optimized with joining temperature of 600°C and pressure of 60 MPa in a vacuum atmosphere.

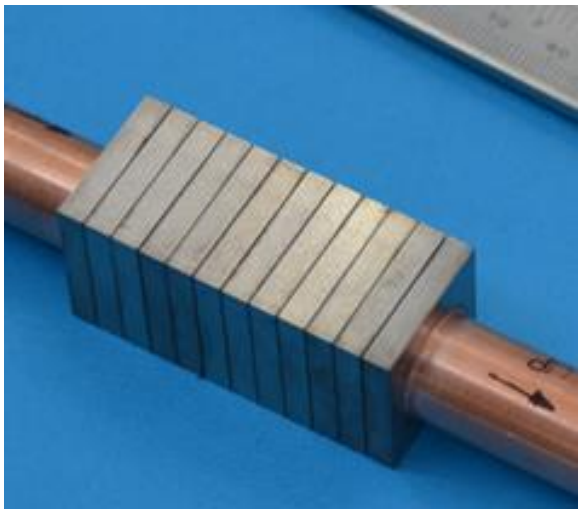

Figure 3: A modified ITER-like mock-up.

Tungsten monoblock with a thin graded interlayer

For enhancing the bonding quality between the armor blocks and the pipe, a compositionally graded thin bond coat (25 μm thick) made of a W/Cu binary pseudo-alloy was used. The primary motivation of this design concept is to replace the thick copper interlayer with a very thin bond coat in order to avoid the potential risk of brittle fracture of thick copper interlayer. Another benefit of this concept is that the surface temperature of the armor is reduced as the distance of heat transport path is shortened by the missing thickness of the interlayer. On the other hand, the absence of an initially soft interlayer might possibly cause bonding defects during fabrication or operation as the thermal stress will not be relaxed so much as a thick Cu interlayer does. This shortcoming should be compensated by a sufficiently high bonding strength, which is actually the major engineering challenge for this concept.

Tungsten monoblock with a thermal break interlayer

A structured copper interlayer is employed for producing a thermal break layer: this approach features axial holes cut into an otherwise solid interlayer to reduce its stiffness and conductance. Various geometric variants of featuring shape were evaluated with an extensive study and the final design of the thermal break interlayer was defined as illustrated in Figure 4. The features could be machined by simple drill or milling operations. In order to reduce thermal stress, the armor blocks were castellated.

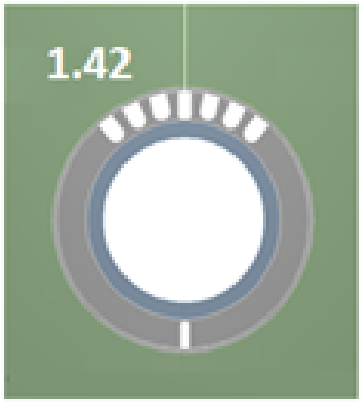

Figure 4: Design of the structured thermal break interlayer.

The underlying idea of this concept is to mitigate the local concentration of heat flux at the cooling pipe by introducing a thermal break between the armor and the pipe.

The major disadvantage of this concept is the fact that the overall temperature field is more elevated compared to the other concepts. As a consequence, tungsten armor is likely to suffer from extensive recrystallization. If the peak heat flux during a stationary operation should exceed 20 MW/m^2, then the structural integrity of the thermal break layer will be affected by strain concentration and fatigue damage.

Tungsten monoblock with a composite cooling pipe

In this concept the divertor target is equipped with a special cooling pipe made of a tungsten wire-reinforced copper matrix (W_w/Cu) composite material. The purpose of using the W_w/Cu pipe is to exploit the high-temperature strength of the composite material and thus to enhance the mechanical stability of the cooling pipe in the hot spot region. The combination of superior strength and high thermal conductivity of the W_w/Cu composite (the copper matrix provides integrity and ductility, but also the medium for thermal conduction) allows the cooling pipe to function as heat sink as well as structural component (containing pressurized coolant water).

Tungsten flat tile with a composite heat sink block

A variant of the so-called flat-tile armor concept (which is considered as an alternative to the monoblock armor concept) consisits in combining a composite heat sink block (surrounding a cooling channel) with tungsten flat tiles as armor. The composite heat sink block is made of a particulate tungsten-reinforced copper matrix composite (W_p/Cu) material. Currently, W_p/Cu composites can be manufactured by well-established industrial production processes. The material properties of the composite are isotropic and can be easily tailored by varying the composition. The flat-tile armor concept with a composite heat sink block offers very high mechanical resilience against structural failure owing to the larger volume (block instead of a pipe) and strengthening of structural material; lower thermal stress; less

complication in fabrication and possibility of in-situ repair. On the other hand high stress concentration are expected at the free surface edge of the bond interface which is likely to initiate cracking

Tungsten flat tile with a W/Cu laminate interlayer

A design where a W/Cu composite laminate layer is employed as a interlayer between the armor tiles and the copper alloy heat sink block is considered in order to solve the issue of stress concentration and cracking at the bond interface edge of flat-tile concept. The W/Cu composite laminate interlayer (roughly 1 mm thick) consists of alternatingly stacked thin (140 μm) layers of tungsten and copper. The combination of the fine-grained tungsten foils and the soft copper layers endows the W/Cu laminate with superior strength and ductility even at ambient temperature. However, the mechanical performance of the W/Cu laminate under neutron irradiation is an open issue.

Tungsten flat tile with a chromium heat sink block

High purity chromium is applied as heat sink block which is joined to tungsten flat tiles on the plasma-facing side and to a copper alloy cooling pipe inside the block. The primary motivation of using chromium as plasma facing component material is to exploit the lower DBTT (250-300°C in unirradiated state) and the extremely low activation characteristic. Indeed the divertor regions out of the strike point are expected to experience only low or medium heat flux (typically 1-5 MW/m^2) but as they are located near the core plasma (distant from the strike point) they are exposed to relatively intense neutron irradiation (recent studies predict irradiation dose rate in the range of 6-9 dpa/y for the copper heat sink of the upper baffle of the targets). In such case the necessity of a radiation-resistant and low-activating material becomes critical.

Helium-cooled steel heat sink

A gas-cooled divertor target is developed as a potential alternative option for the optimistic case that the peak heat flux on the target can be reduced down to 4 MW/m^2. Helium-cooling offers essential advantages over the water-cooled: no corrosion of cooling channel; no transmutation of coolant; no abrupt change in heat transfer due to phase transition; no risk of volatile oxidation of tungsten wall in the event of accidental coolant ingress; higher coolant temperature; reduced irradiation damage of structural materials. On the other hand, the significantly limited power handling capability is the major shortcoming preventing this concept from being considered as a competitive option for the high heat flux applications.

The considered helium-cooled target features a tungsten monoblock type with a cooling pipe equipped with a perforated tubular cartridge inside the pipe for gas jet impingement (see Figure 5). The heat sink material used for the pipe is EUROFER97 steel. Analyses show that the maximum temperature in the steel pipe and the tungsten armor reaches 670°C and 1070°C, respectively, when the surface heat flux is as high as 5 MW/m^2: this indicates that if ODS EUROFER steel is used as the pipe material, helium-cooled targets could potentially

withstand up to 4-5 MW/m^2 (the maximum allowable service temperature of ODS EUROFER steel is roughly 650-700°C). Here, 300°C was taken as the coolant inlet temperature in order to maintain the operation temperature of the structural component (i.e. pipe) above the DBTT of EUROFER97 steel (roughly, 300°C).

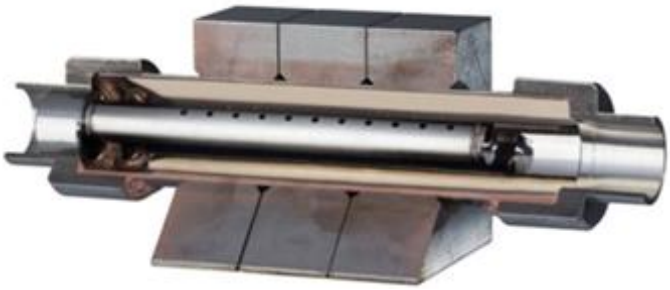

Figure 5: Fabricated helium-cooled divertor target mock-up.

As an interim, untill the avilbilty of the DEMO Design Criteira, both WPBB and WPDIC have proposed interm design rules and methodologies to progress the designs. WPBB are working closly with the Fusion for Energy Test Blanket Module programme and using RCC-MRx rules and self developed analysis methodology (EFDA_D_2MXWTC, JA report). WPDIV have made adaptations initially based around the SDC-IC and have a proposed procedure for analysis (EFDA_D_2CYH6Q, EFDA_D_2MDFQB). The proposed method for desing anlysis from WPBB and WPDIV are closley reviewed by the WPMAT Eddi team to ensure consistence with DEMO Design Criteria developments.

3. Status of Materials Database & Design Rules

3.1. Materials Data Base and Property Handbook:

Although not the main subject of this report, it is appropriate to review materials database and materials property handbooks for DEMO. Materials Property Handbooks (MPH) contain bounded materials data generally of the average and minimum property values for materials based on the statistical analysis of fully screened and high provenance materials testing/inspection data. The data in Materials Property Handbooks are the key input and the bases for the material appendices in the respective codes (e.g. Appendix A in ITER-SDC), where they are differently presented and used to calculate engineering data and limit data (Design Allowables), which include safety factors, specific to each set of Design Criteria. At present, based on the needs of design assessment methodology to be used, materials properties in the MPH cover a range of areas including but not limited to: composition, physical properties (e.g. density), thermal properties (e.g. thermal conductivity), mechanical properties (e.g. tensile strength), and magnetic properties. The materials properties will have to cover the properties over the designed operational environment including but not limited to temperature and neutron fluence. A particular environment of fusion plasma-facing and in-vessel components is the fusion neutron spectrum. This varies throughout the components, which will certainly have significant impact on modification and degradation of properties, damage and failure modes (Bloom, 2007).

All product forms (e.g. rolled plate/bar) and joints (e.g. weldment) to be used on designs need to be separately evaluated to determine if their properties are different. Wherever properties are different, separate sections to the MPH or modification factors (e.g. a reduction in tensile strength of 20% welded materials) need to be implemented in the code.

Within the context of the EU DEMO design, a dedicated DEMO materials database, the DEMO MPH, has been initiated. The Appendices to the DEMO Design Code need to be produced, which may include issues such as “code qualification” of new materials (like EUROFER97), or types of material (fiber or particle reinforced options of the baseline materials). The approach currently followed by F4E for EUROFER97 is a model and blue print for future activities, indicating in particular the complexity, the long lead time and resources that must be spent. The initial aim is to focus on the ***baseline*** structural or armor materials anticipated in the breeding blanket and divertor components, specifically: EUROFER97 (main structural materials for BB and DIV cassette), Copper-Chrome-Zirconium (CuCrZr; main heat-sink/structural material for DIV target) and tungsten (main armor material for DIV targets and First Wall). Presently, the MPH required for DEMO is far from complete, and there is significantly less than half of the required materials data for EUROFER97, CuCrZr, and Tungsten. Technically, despite a significant volume of work, most of the materials database for the un-irradiated state of the materials can be obtained using conventional testing. However, there are several key areas within the context of DEMO that need to be addressed, including but not limited to:

- Acceptability of small scale test techniques required for n-irradiation campaigns.
- Inclusion of advanced/novel test data specific to new design criteria.
- Access to sufficient irradiated materials tests data.
- Full knowledge of the joining conditions to be utilized and supporting test methodologies for the characterization of multi-materials interfaces.
- Evaluation methodologies for unique aspects of high heat flux and plasma erosion.
- Determination of corrosion and intermetallic formation due to coolant and breeding materials.
- Evaluation of brittle materials, requiring Weibull statistics.
- Determination of a baseline materials along with supporting industrial production assessments.

This is not an exhaustive list of the critical issues, but the above aspects highlight the challenges that need to be addressed in order to provide the necessary data for the design-by-analysis procedure. Work is ongoing within the EUROfusion materials program to address these points and provide data founded on fission irradiation campaigns.

A specific area of uncertainty is the difference in neutron spectra between fission and fusion. The current irradiation database is derived from campaigns in fission reactors, while the data is needed in the fusion neutron spectrum. The high-energy tail in fusion (originating from the 14 MeV neutron reaction) results in an order of magnitude higher probability for inelastic (nuclear) reactions, where alpha-particles and protons manifest as the gaseous elements helium and hydrogen in the structure. As an example, in an Fe-First Wall, the production rates of He and H, respectively, are 10 and 40 times higher in a fusion spectrum compared to fission reactors. The strategy is to gather data of irradiated materials (MPH and deduced limit data) from fission reactors, and implement later "best-estimate" or "conservative" modifications of the fission data based on "validation" and "verification" together with dedicated modelling.

There is then a need for (further) irradiation experiments to address the synergies of neutron damage to the structure and superimposed He, H, tritium effects. This is highlighted as a key issue to get the *proper material data* and respective appendices.

3.2. ITER Structural Design Criteria for In-Vessel Components (SDC-IC)

From the beginning, the structural design of in-vessel components for fusion reactors has been based on the ASME code – Section III Division 4, and the AFCEN – RCC-MRx. There have been improvements over the years, primarily related to embrittlement and high temperature design, but the spirit of the current codes comes directly from these earlier ones. In all cases, these codes comprise a set of rules that permit the designer to choose materials and geometric parameters to ensure that a structure will survive the prescribed

loads for the desired life of the component. The codes begin with an identification of the service limits relevant to a component, classify the stresses in the component according to whether they are self-limiting, and compare these stresses to allowable stresses, depending on the material, temperature, etc. If the rules are satisfied, then the designer is assured that the operation of the component will be safe. Unfortunately, in simplifying this process, the codes introduce conservatism and lead to excessive design margins.

The Section III of the ASME Code was added in the 1960's to address the needs of the emerging nuclear power industry. The Code considers stresses due to pressure, thermal stress, and geometric discontinuities, along with creep rupture. It explicitly leaves consideration of fracture to the designer and does not address ductility changes due to irradiation. A related set of rules is contained in ASME Subsection NH (Rules for Class-1 elevated temperature nuclear components). These rules were developed for the liquid metal fast breeder reactor program and they cover 304 stainless steel (SS), 316 SS, 800 H, and 2 ¼ Cr-1 Mo, with allowable temperatures as high as 800 °C, depending on the alloy. A key difference between this subsection and the original ASME code is that when creep strains are considered, it is done through inelastic analysis, rather than through the allowable stress coupled with an elastic analysis. NH provides design rules to account for potential high temperature damage mechanisms such as creep rupture, excessive creep deformation, creep buckling, and cyclic creep ratcheting. It does not require consideration of brittle fracture, other than in the case of embrittlement in ferritic steels. This subsection uses a bilinear creep and fatigue damage summation rule that most would consider overly simplistic. For Generation IV fission reactors [3], there is a need for additional materials to be included in the database in NH, as well as consideration of higher temperatures for some designs. There also is a need for new design rules for materials which don't exhibit primary or secondary creep (such as Inconel 617), preferably also incorporating unified inelastic models combining creep and plasticity.

The ITER Structural Design Criteria (ISDC) are based on the ASME rules, with significant additions addressing some features which are expected to be more prominent in fusion reactors, relative to fission reactors. These new rules address the following damage modes: immediate plastic collapse, immediate plastic instability, non-ductile modes, immediate plastic flow localization, immediate local fracture due to exhaustion of ductility, fast fracture, thermal creep, ratcheting, fatigue, buckling, and irradiation effects (including irradiation-induced creep, swelling, and property changes). A key element of these more modern rules is the consideration of ductility measures that permit quantitative assessment of the safety margins in the context of localized failure. Typically, this results in allowable stresses which are adjusted to account for materials with low ductility. A second key element in the ITER Design Rules is fracture, which is not explicitly considered in current codes. In this case, the fracture toughness accounts for both temperature and irradiation effects and a safety factor is applied to the allowable stress intensity factor. Creep deformation is also treated more comprehensively in the ITER rules. In current codes, creep is only considered in the sense that the allowable stress is determined, in part, by creep rupture behavior. However, there

is no need to analyze creep strains in any structure. The ITER rules account for elongation at rupture, strain at rupture, average and minimum time to rupture, and usage fraction rules based on rupture time and strain. The rules also contain a significant discussion of viscoelastic deformation. This is employed in cases of large creep strain, including irradiation creep strain, and there are cases covering loss of membrane ductility and plastic collapse.

A summary of the current ITER Structural Design Criteria (SDC) for In-vessel Components (IC) is given in appendix A.

4. Limitations and challenges of rules and analyses

The origin of a considerable amount of work to be done to converge to the best DDC is the history of current frameworks. The criteria formulated in ASME and RCC-MRx typically were written for fcc-materials (such as stainless steels) and approaches and concepts were deduced appropriately, whereas DEMO blanket materials are bcc (such as FM steel EUROFER97). FM steels often exhibit cyclic softening, whereas SS is cyclic hardening, and the yield strength is already very high, whereas SS typically shows lower yield, but very pronounced strain hardening.

Other factors incorporated into the ITER design rules include treatment of welds, corrosion, and erosion, consideration of layered structures, structural discontinuities, and joints (welded, brazed, and bolted joints). Despite the extensive effort put into developing high temperature design methodologies, there still are deficiencies in the design codes, leading to substantial uncertainties in the predicted viability of fusion components. Some examples of phenomena which are not adequately addressed in the current ITER SDC include:

1. The rules for combined creep and fatigue damage are simplistic and should be updated with a more physics-based criterion, which will likely have to be material-specific and account for environmental effects (ITER Organization, 1998).
2. Rules for addressing the requirements for fusion specific transients, such as disruptions and ELMs, must be included. The current ISDC mentions these, but the physics understanding is not at a level that permits these to be addressed in detail now.
3. There is still debate regarding the difference between in-reactor deformation and post-irradiation tests. There is some indication that in-reactor tests will lead to larger predicted rupture strains as compared to those found in post-irradiation studies (ITER Organization, 1998).
4. For most materials, the data to support design is not adequate, even in the unirradiated state and with existing design rules. As the design rules evolve, new data will be required for all materials.
5. Criteria for bellows (to accommodate thermal expansion) must be added to current Codes.
6. The new design criteria, primarily those rules that prevent excessive deformation and ratcheting, must be tested for both unirradiated and irradiated materials at elevated temperatures.
7. Criteria for ductile fracture in high temperature environments with substantial amounts of He in the material must be developed and tested.

5. A review of the existing DEMO Design Criteria

5.1. Summary of impacts from currently considered DEMO Roadmap

To deliver an integrated DEMO design, a phased and structured design process has been defined. This consists in the following design phases, with key C&S related activities highlighted:

- Pre-Conceptual Design Phase, till 2020
  - Define DEMO Architecture.
  - Define requirements.
  - Define 2 DEMO plant concepts.
- Conceptual Design Phase, 2020 – 2027
  - Develop and select single architecture by 2025.
  - Perform cost safety and feasibility assessments.
  - Confirm remote handling strategy through test-rig and trial demonstrations.
  - Perform a Concept Design Review.
- Engineering Design Phase, 2027 – 2037
  - Perform preliminary and final design reviews for all systems.
  - Engage regulator and initiate licensing by 2032.
- Site selection and preparation, 2035 – 2039
  - Engage national regulator
  - Ensure local regulatory requirements are identified
- Plant Construction Phase, 2039 – 2050

The realization of a successful DEMO would require the resolution of several key challenges. The DEMO roadmap attempts to address the key challenges through the initiation and coordination of 8 Missions summarized below:

- **M1. Plasma regimes of operation**
- **M2. Heat-exhaust systems**
- **M3. Neutron resistant materials**
- **M4. Tritium self-sufficiency**
- **M5. Implementation of the intrinsic safety features of fusion**
- **M6. Integrated DEMO design and system development**
- **M7. Competitive cost of electricity**
- **M8. Stellarator**

Although the development of DEMO Design Criteria has links with all the missions, it is directly related to M2, M3 and M4.

It is worth noting that in the executive summary it is mentioned that: “The mechanical and thermal properties of materials can change substantially under neutron irradiation. Therefore, updated design codes and structural criteria standards are needed based on new data interpreted with advanced theory-based models to allow the highly-irradiated components of DEMO and power plants to be designed."

5.2. Nuclear Regulator

In general, C&S are regularly used to demonstrate an acceptable level of safety conformance to the licensing regulator. As such, it is important to understand the likely licensing regime for DEMO. In doing so, the “likely licensing regime for DEMO” report was reviewed, with key points listed here:

- Even though ITER is licensed in France under existing laws, in most countries it seems likely that new regulations would have to be enacted in order to license a fusion power plant on the scale of DEMO.
- Two important regulatory principles are that regulations should be *targeted* and *proportionate*. This may mean that any new legislation introduced to license fusion plants would consider the reduced hazard level of fusion compared with existing fission reactors; at the very least it will be suitable for fusion, taking account of the specific hazards and safety characteristics, rather than trying to adapt regulations written primarily for fission reactors.
- National regulators are unlikely to want to consider issues of fusion licensing in any detail until a real fusion power plant seems much closer and some firm proposal can be considered. Regulators are generally not inclined to give advice about what would or would not be acceptable, but prefer to consider and examine a firm proposal.
- The move towards harmonization of nuclear regulation across Europe is useful because it eliminates uncertainty about differences between national approaches, when considering the future licensing of DEMO.
- The documents of WENRA, which is leading this harmonization, give useful insight into the direction in which European nuclear regulation is going. There is a strong emphasis on Defense in Depth, which is also a key principle in the DEMO safety approach.
- As far as can be discerned at this stage, the safety approach being adopted for the EUROfusion DEMO project is consistent with the developing nuclear regulatory approach in Europe.
- The French nuclear regulator, ASN, is unique amongst regulators worldwide in being one that has licensed a nuclear fusion facility, ITER. They have obtained an understanding of fusion science and technology and the related safety issues. Their technical advisors, IRSN, have developed a comprehensive understanding of the technicalities of ITER systems with respect to safety and environmental performance.

From this report, it was highlighted that currently regulators are reluctant to provide a clear indication of the required licensing regime of DEMO, mainly due to the infancy of the project.

In addition, as a site has not yet been identified, it is not clear as to which regulator needs to be consulted for advice. This is reflected in the Fusion roadmap, where the engagement of the regulator is expected in 2032. However, in the short term, an indication of the likely licensing regime is required. This can be covered by using ITER as a model. The French regulator classes ITER as an Installation Nucleaire de Base (INB) and as such it treats ITER in the same way as every other Nuclear facility in France. If DEMO was going to be built in France (site currently unknown) then following the ITER licensing experience would be appropriate. However, there is a possibility that DEMO could be built elsewhere in Europe, as such other European regulator licensing regimes need to also be considered. In most countries, it seems likely that new regulations would have to be enacted to license a fusion power plant on the scale of DEMO. This may mean that any new legislation introduced to license fusion plants would consider the reduced hazard level of fusion compared with existing fission reactors; at the very least it will be suitable for fusion, taking account of the specific hazards and safety characteristics, rather than trying to adapt regulations written primarily for fission reactors.

Despite the large number of unknowns remaining with regards to a likely regulator regime, several knowns exist:

- All relevant laws and regulations must be respected.
- However, the regulator may not impose specific codes and standards, requirements, etc.
- The operator applying for a license must make their own choices and then ***demonstrate*** to the regulator that these are appropriate and will guarantee safety objectives are met.

The regulator will concentrate its effort on safety related systems. As such the safety classifications of the DEMO Blanket and Divertors shall provide an indication of the likely C&S the regulator is intending to see.

5.3. Safety Classifications

Safety classifications are set by nuclear regulators based on the safety importance of the component under considerations. A brief description of safety classifications is provided in Appendix B.

Currently the classification of the DEMO Divertor and Blanket are not defined, although it is anticipated they will not be SIC1 components. The classification by regulator of the Divertor and Blanket components, by the national regulator of the country where EU-DEMO is constructed, may subsequently change the necessary regulation applied, the design codes used and potentially required designs changes.

5.4. Codes and Standards

Standard: A standard consists of technical definitions and guidelines that function as instructions for designers/manufacturers and operators/users of equipment. Standards can run from a few pages to a few hundred pages and are written by professionals. Standards are considered voluntary because they are guidelines and not enforceable by law.

Code: A code is a standard that has been adopted by one or more governmental bodies and is enforceable by law.

Currently, the two major Nuclear Codes come from ASME and AFCEN, neither of which fulfils the needs of DEMO. This is the primary reason as to why the need for DEMO Design Criteria was identified. However, the ideal solution could be to integrate the development of the DDC into both AFCEN and ASME code suites. From an idealistic standpoint, the creation of an International Fusion Code (ISO) would be highly beneficial and should be explored as an option.

Within ASME and AFCEN the key development areas within the codes that are considered optimal for integration of a fusion specific code or fusion specific aspect are: AFCEN – RCC-MRx and ASME – Section III Division 4. Along with interactions with IAEA on an international fusion code, interaction with ASME and AFCEN on development and integration of the RCC-MRx and ASME Section III Division 4 are being pursued.

5.5. DDC Mission Statement

To develop a European DEMO, key engineering challenges must be resolved including the development of viable plasma facing component designs. These components have conflicting design constraints and requirements that must be mutually satisfied. They are required to maintain structural integrity while operating within unique and harsh fusion environment. Currently, existing Nuclear Codes do not meet the needs of the DEMO Fusion community in number of key areas:

- Insufficient coverage of damage mechanisms in end of life conditions.
- Insufficient coverage of modifying effects.
- Insufficient irradiated material data.
- Restrictive design space, making it challenging to develop a design solution.
- Design rules have not been developed for complex 3D structures and modern FEA.

As such it has been recognized that a systematic approach to design verification will be required, drawing on industry precedence and best practice. The target for the DDC is to develop a new set of design criteria to enable the design of DEMO plasma facing components (Blanket and Divertor) including unprecedented environmental conditions, going beyond any existing framework.

5.6. DDC structure outline and milestones

From a review of the EUROfusion plans two key milestones need to be met:

- Deliver validated and tested design criteria for the BB and DIV teams by June 2023.
- Review integration of the DEMO design criteria into a Nuclear Code that covers the BB and DIV teams by June 2027.

The design assessment of the DEMO PFC's intends to demonstrate that the component shall retain its structural integrity for the required operational duration. Therefore, the potential damage mechanisms need to be identified and verified that they do not cause an unplanned failure. Although it is recommended that the PFC should be modelled and assessed in its entirety, each of the elements will not be subject to the complete range of damage mechanisms. The following Table 2 highlights the damage mechanisms that need to be assessed for each particular element and therein the damage mechanisms are divided into three groups: (1) Monotonic damage based on strength; (2) Monotonic damage based on fracture; and (3) Cyclic damage based on both strength and fracture.

Table 2: Damage & Failure Mechanisms of Structural Components

Damage Mechanisms	**Structural Element**	**Armour Element**	**Joint Element**
Monotonic Damage – Strength-Based			
(1) Plastic Collapse		Potentially relevant	TBC
(2) Plastic Flow Localization		Potentially relevant	TBC
(3) Ductility Exhaustion		Potentially relevant	TBC
Monotonic Damage – Fracture-Based			
(4) Fast Fracture (Brittle or Ductile)			Potentially relevant
(5) Slow Fracture by Creep		Potentially relevant	TBC
(6) Stress Corrosion Cracking			
Cyclic Damage –Fracture-Based			
(7) a-Ratcheting: Fracture; b- Ratcheting: Collapse; c- Ratcheting: Exhaustion.		TBC	Potentially relevant
(8) Fatigue Crack Growth			
(9) Creep-Fatigue Fracture			

6. Hierarchical Multiphysics-Multiscale Approach

6.1. The Role of Multiphysics in Design

Multiphysics Finite Element simulations are becoming common tools of design in many fields of science and technology. The implementation of multiphysics requires some skills in the design approach. First, the type of physics equations that must be coupled for a faithful representation must be selected. Then, one must decide on the possibility of one-way versus two-way coupling. If one of the physics modules has a small influence on another, a one-way coupling scheme is appropriate. Strong coupling, on the other hand, requires non-linear solvers and more iterative methods of modeling. In the case of designing thermomechanical components, as is the case with DEMO BB/DIV elements, one should couple heat transfer in fluids with fluid flow simulations, and those again should be coupled to heat transfer in solids, which is finally coupled with structural analysis. Turbulent fluid mechanics simulations for large modules become challenging, and one may have to resort to decoupled solutions between the fluid flow module and the heat transfer in fluids module via appropriate heat transfer correlations. Because of the computational challenges in non-linear structural design that include plasticity, creep, and damage, the multiscale design process now would have to rely on a purely elastic analysis. The main purpose is to ascertain the global stress distribution in large structural components, and to furnish boundary conditions for specific critical regions that can be identified from the elastic analysis alone. With conservative design limits and additional post-processing of the FEM data, the designer can have an "enhanced elastic analysis" in hand. Meeting design criteria through this step alone can be very beneficial in the process of design optimization and selection between alternatives.

Figure 7 and 7 illustrate the relationship between the two design procedures of "Multiphysics" and "Multiscale". It may be envisioned that only multiphysics will be required in the future, if we have sufficient computational capabilities and software development to incorporate all levels of multiscale analysis into multiphysics. However, this prospect may present itself far into the future, and thus has to be abandoned now in favor of the more realistic approach suggested here. As will be described next, the multiscale approach will be performed at three levels of analysis, with more details of the physical mechanisms and material behavior, as moving from the coarsest analysis tool (level-I) to the highest resolution analysis tool (level-III). Therefore, it is anticipated that a full multiphysics simulation would include level-I type analysis (Elastic, or E), which is entirely elastic with enhancements that reflect aspects of material ductility. The multiscale approach would then focus on level-II (Plastic, or P) and level-III (Microstructure, or M), as can be seen schematically in 7.

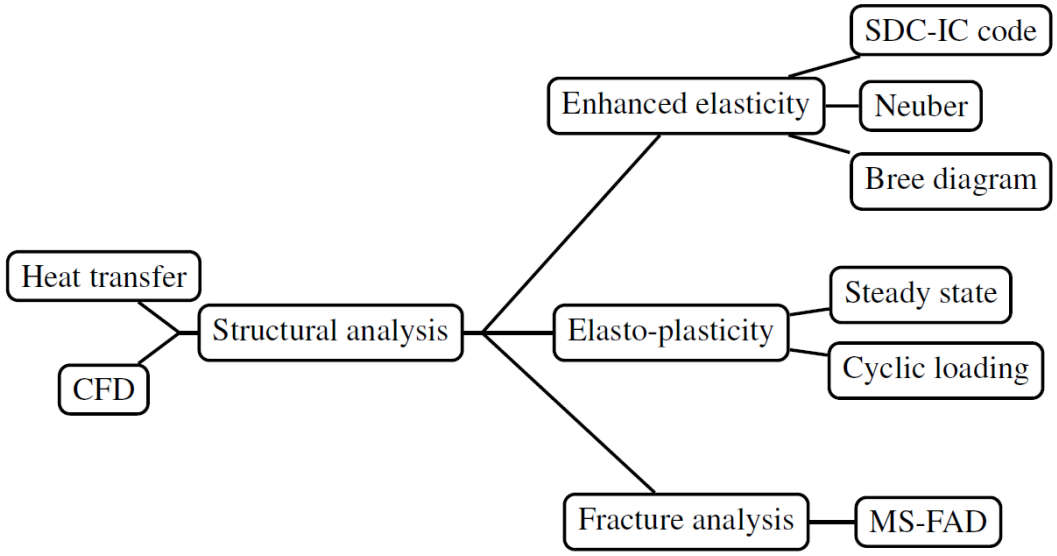

Figure 6: Schematic Illustration of the Coupled Multi-Physics-Multiscale Methodology.

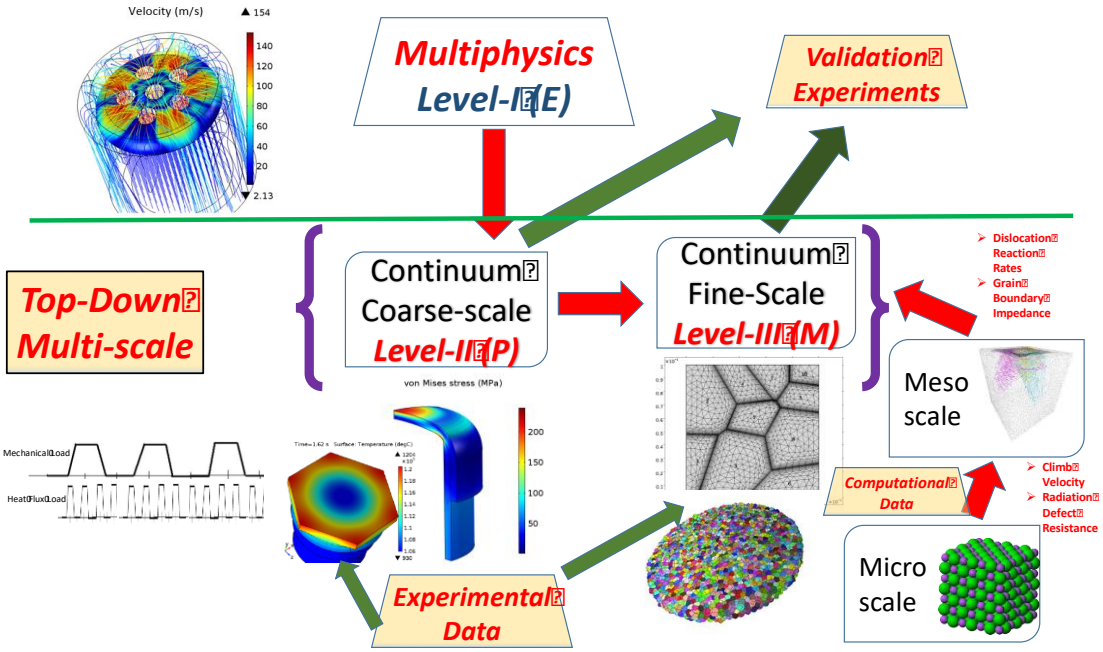

Figure 7: Illustration of the connection between "multi-physics" design, and "Multiscale" analysis.

6.2. Overview of the Hierarchical Multiscale Design Methodology (HMDM)

The Hierarchical Multiscale Design Methodology (HMDM), illustrated in Figure 7, is composed of three levels of analysis, each incorporating increasing fidelity of physical mechanism representation, as we proceed from the top level-I (E) towards level-III (M). The transition requires some judgement on the representation of the appropriate geometry element, operating environment, boundary and initial conditions. Tractability of the calculations will depend on these initial judgements. For example, at Level-II (P), detailed cyclic plasticity simulations can be performed on small representative volumes that should be connected to a few critical regions, which have been previously identified at the coarser level of analysis (E).

It is envisioned that the designer or analyst will first perform full structural analysis, coupled with other relevant multiphysics simulations at level-I (E). At this stage of analysis, one would have two possible options: (1) a deterministic analysis option for critical components that must be designed for safe-life; and (2) a probabilistic analysis option, exercised for elements that can be designed as fail-safe. An example here would be the design of armor and protective coatings on divertor components. At this level of simulations, the designer would "enhance" the elastic analysis via two routes: (1) increase the allowable stress limits to include some measures of ductility (as is the case with the current ITER SDC-IVC), and (2) update the elastic solutions using approximate methods, such as those proposed by Neuber for the influence of ductility on fatigue around notches and stress concentration zones (Neuber, 1961).

6.3. Level-Ia: Deterministic Enhanced Elastic Analysis

At this highest level of analysis, the solution of the elastic field in a representative section of the structure is obtained numerically with the Finite Element Method (FEM). The solution would be based on elasticity theory, and would be coupled with other important elements of multiphysics (fluid flow, heat transfer, thermal expansion, electromagnetic forces and accumulation of radiation defects). The results of this step must be interpreted in terms of potential failure mechanisms. It would seem inconsistent that while material failure implies plastic deformation and fracture, there is no information relating to material behavior and damage mechanisms that appears at this stage. However, in practice this stage is going to represent the main step in the design process, since we already have many of the computational tools available, which are required for performing reasonably accurate predictive simulations. Using also the suitably quantified data derived from ion and neutron irradiation experiments, it appears possible to develop a predictive approach for carrying our engineering studies in a comprehensive manner, deriving stress and strain fields everywhere in the engineering structure of the reactor under a broad range of assumed operational conditions, and hence enabling fast computational testing of a range of design concepts associated with realistic neutron and thermal loads.

A self-consistent algorithm for the assessment of design concepts can be described by a sequence of steps as follows:

- An assumed engineering design of a power plant is represented by a finite element model (FEM), where information included in the definition of finite elements includes data on the temperature-dependent elastic and thermal properties, the shear modulus of the material, its thermal conductivity coefficient, the temperature-dependent bulk modulus etc.
- A model for plasma, consistent with the power plant design, is assumed and the intensity of heat and neutron sources are computed.
- These sources provide input for heat and neutron transport simulations, which determine, in a self-consistent way, the distribution of temperature and neutron fluxes everywhere in the structure of the power plant.
- The neutron fields computed from neutron transport simulations provide input for the evaluation of local rates of defect production everywhere in the power plant structure.
- Microstructural evolution models, which use the rates of defect production and temperature as inputs, produce information about the local volume densities of defects at various locations in the structure.
- The density of defects provide input for FEM calculations computing stresses and strains in the structure. The FEM model use elastic equilibrium equations treating gravity, electromagnetic forces, thermal expansion of materials, as well as volumetric forces resulting from the accumulation of defects.
- The local density of defects is used as input for simulations re-evaluating local thermal conductivity, and the distribution of temperature in the reactor structure.
- The above model is evolved through time, until stresses or strains reach a critical level. The critical level is decided using information obtained from experimental tests, for examples values of the UTS or similar criteria. The simulation is now stopped and results analyzed, providing input for the re-evaluation and optimization of the power plant design concept.
- Go to step 1 and iterate until a satisfactory design solution is found.

The algorithm is going to require information derived from variable temperature ion and neutron irradiation experiments, to determine and verify the rate of accumulation of defects in materials, derived from the microstructural evolution model at step 5 of the above algorithm.

It is appreciated that further effort would be required to translate the results of elastic analysis described above, to something that can be used to specify and determine the specific material failure mechanisms. This is precisely the idea of “enhancing” elastic analysis. One would want to use the results in some way! This has been accomplished in the mechanical design field along three directions:

(1) Selecting specific critical paths in the structure, post-processing the FEM data to break it down to membrane, bending, thermal, and peak stresses, and then compare those to allowable levels of stress. Although the effective values of membrane, bending, thermal, and peak stresses are computed elastically, the corresponding allowable stresses are derived from experimental tests and experience, and include the effects of complex variables, such as stress triaxiality, and the available ductility of the material. In this giant step, elastic analysis would be related to failure mechanisms that are the results of plastic deformation and fracture processes. This process has been the basis of the ISDC-IVC, as briefly discussed in Appendix A.

(2) The second direction was pioneered by Neuber within the context of fatigue design. In this approach, again, a post-processing step is made to re-compute the stress and strain field via approximate energy conservation principles, whereby the uniaxial stress-strain curve is used to re-compute stresses in the plastic regime approximately, using available elastic information alone and a conservation of energy principle. In this fashion, elastic stresses (which tend to be overestimated at high loads) would be reduced, and the elastic strains increased to mimic the results of full-fledged plasticity. An example of this method is shown to determine fatigue failure in an entire car body, with the Neuber plasticity correction at critical notches and stress concentration zones (Neuber, 1961).

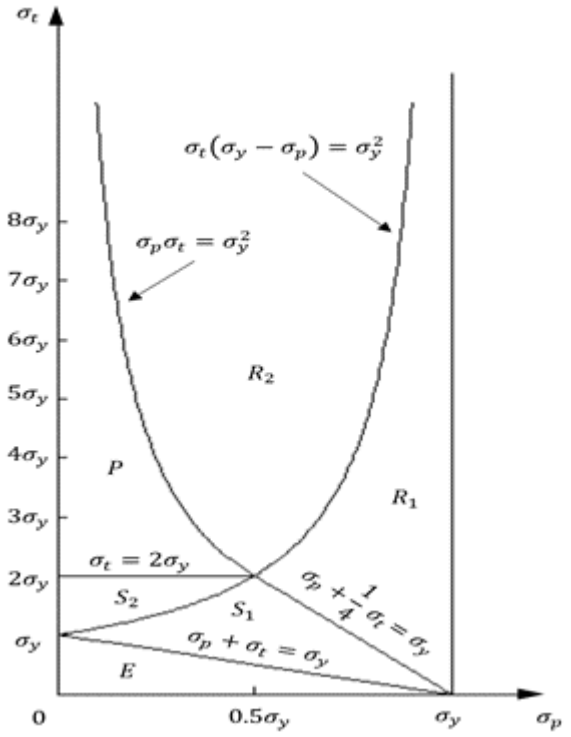

Figure 8: Bree diagram for limit analysis of cyclic perfect plasticity.

(3) The third area of enhancement is performing plastic limit analysis. In this case, the material can be assumed to be elastic-perfectly plastic (and in some cases with linear

hardening behavior), and the plasticity analysis is performed "post-mortem." The stress can be divided into membrane and bending components that can include thermal stress gradients. Limit analysis can then be performed following the approach of Bree (Bree, 1967). The membrane stress from an FEM calculation would be equivalent to the pressure (mechanical) stress σ_p in Bree's analysis, and the bending stress (if it is cyclic) can be equivalent to the thermal stress σ_t. A Bree diagram (see Figure 8) can be constructed to determine the expected regimes of ratcheting, elastic shakedown, and plastic behavior, and to calculate the accumulated plastic strain from cycle-to-cycle in an approximate manner.

The six different regimes based on the Bree analysis and used in the ASME Design Code [(1) elastic E; (2) plastic P; (3) shakedown S_1; (4) shakedown S_2; (5) ratcheting R_1; and (6) ratcheting R_2 are shown in Figure 7.

6.4. Level-Ib: Probabilistic Enhanced Elastic Analysis

While the above analysis is based around a deterministic approach, where bounding data values are used thus providing a large level of inbuilt conservatism, a growing trend in analysis is to use a probabilistic approach. Probabilistic approach accounts for the uncertainty in the data to provide reliability factors, rather than bounding data, and reduced conservatism in design. Reliability factors, which provide predictions on the probability that the component will not fail, can also allow designers to evaluate the margins of component life. This approach may not be applicable to safety critical systems at present but may be more applicable to armor materials, where the failure of the component does not imply immediate safety concerns.

It is proposed that if a non-safety critical component does not pass level 1 (Advanced Elastic analysis) designers may choose to move away from a deterministic approach and adopt a probabilistic approach.

There are several different probabilistic design assessment options available, ranging from partial probabilistic to fully probabilistic. The most established being the Partial Factors approach. This approach has been extensively and successfully used in the Civil Engineering industry for several years, and as such now exists in the associated Codes and Standards. This technique has also now made its way into the appendix of EN13445. The more advanced fully probabilistic techniques are also gaining traction with ASME developing a System Based Code that utilizes probabilistic techniques.

Significant adaptations to the existing probabilistic assessment methods will need to be prepared for its application for fusion components but it represents a method to reduce the conservatism in design that is appropriate where there are high uncertainty levels.

6.5. Level-II: Elastoplastic Analysis

At level-II of multiscale modeling, a few critical regions are selected from the elastic analysis of level-I, where there is danger of damage accumulation in the form of plastic strain or fracture. The model would be built up from 3-D configurations of a critical region experiencing the highest stress distributions. The boundary conditions can be imported in the form of tractions and displacements from level-I, and imposed on the geometric model. The designer would then proceed with continuum elasto-plastic analysis to study the effects of cyclic loading on the accumulation of plastic strain (ratcheting), the possibility of Low Cycle Fatigue (LCF) crack growth, and the possibility of crack propagation by fast fracture (Aktaa, Kecskes, & Cismondi, 2012). One difficulty in this step is the correct coupling between level-I and level-II, because stress relaxation due to plastic flow in level-II would result in changing the stress distributions around the surfaces where the critical region has been extracted from the larger model of level-I. Iterative schemes would be necessary at this stage, as calculations proceed in level-II, where one would expect larger plastic strains with each cycle and further stress relaxation that needs to be compensated in level-I. Details of such multi-grid methods are discussed by (Huckbusch, 2013) and illustrated in 9.

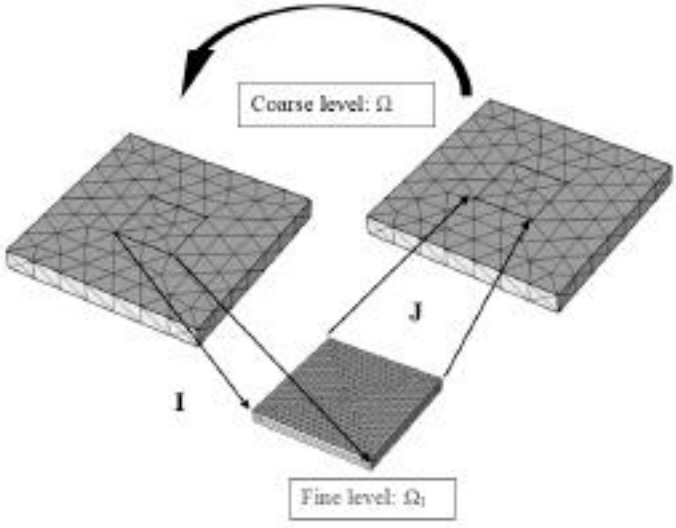

Figure 9: Illustration of the multigrid method

While multigrid methods will be useful in identifying critical regions of the structure that need further detailed non-elastic analysis, they are not generally utilized in coupled global elastic to local non-elastic analysis in design level-II. For that purpose, a global elastic analysis must be coupled to a local elasto-plastic analysis. A self-consistent method, such as that proposed by Park (Park & Felippa, 2000), can be used. The method is based on the introduction of interface Lagrange multipliers in a variational energy principle, as illustrated in Figure 10. The interface is treated by introducing a displacement and Lagrange multipliers

in an additional potential energy that can be minimized and solved for matched displacements and tractions (Huang, 2018).

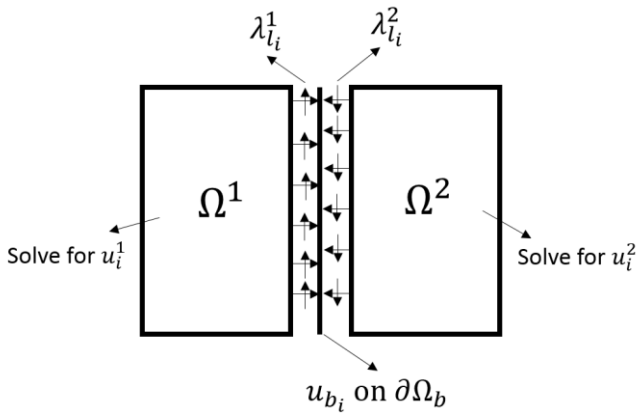

Figure 10: Localized Lagrange Multiplier Field at the Interface between Global and global and local regions.

It is recommended that the mechanical properties data of the material be represented in simplified functional forms. Properties would be functions of temperature, strain rate, and neutron radiation fluence. For example, the stress-strain curve can be represented by four parameters: the elastic modulus, the yield stress at 0.2% strain, the tangent (plastic) modulus, and the ultimate strength. These four parameters would be functions of temperature, strain rate (if any), and neutron irradiation fluence. The fully plastic analysis would then be possible for beginning of life to end of life of the component. Following cyclic elasto-plastic calculations, the designer would be faced with making a judgement on the potential for failure in this critical region. A "damage assessment" phase would then follow from the results of level-II calculations.

6.6. Failure Assessment at the Continuum Scale

Material-Specific Failure Assessment Diagram (MS-FAD)

The Failure Assessment Diagram (FAD) can be a valuable tool for determining the structural integrity of a component containing a crack (Ainsworth, 1993) (Budden & Ainsworth, 2012). The abscissa of the FAD is the plastic collapse ratio, denoted by L_R, which is the ratio of the applied stress σ_a to the yield strength S_y. The ordinate of the FAD is referred to as the brittle fracture ratio K_r, which, as the name suggests, is the ratio of the stress intensity factor K to the fracture toughness K_c of the material. A typical FAD is depicted in 11. Note that points that lie inside the FAD curve correspond to stable cracks whereas points that lie outside the curve indicate cracks that will cause component failure.

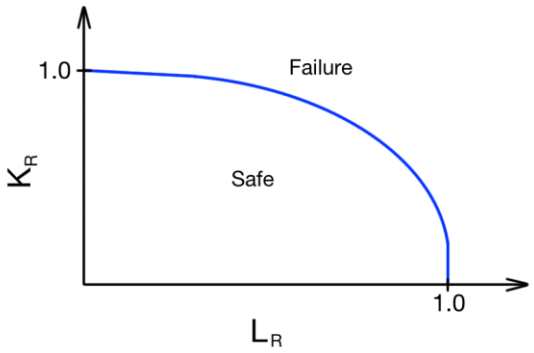

Figure 11: Typical FAD diagram.

A useful extension to the standard FAD is a material and geometry-specific FAD (MS-FAD) that can be generated if an FEA model of the component and stress-strain data for the material are available. In the MS-FAD, the plastic collapse ratio L_R becomes the ratio of a reference stress σ_{ref} to S_y. To find the reference stress, it is necessary to calculate a geometry factor F. The ratio between the elastic J-integral J_{elast} and the total J-integral J_{tot} is required to do so. This can be obtained using elastic and elastoplastic FEA models of the component.
The geometry factor F is defined as the ratio of S_y to the nominal stress σ_{nom} required for plastic rupture. That is, one must find σ_{nom} at $L_r = 1$. The geometry factor is then obtained by the relationship $F = S_y/\sigma_{nom}\,|_{L_r=1}$. In the elastoplastic J-integral example in Appendix A, the geometry factor is found to be F = 2.52.

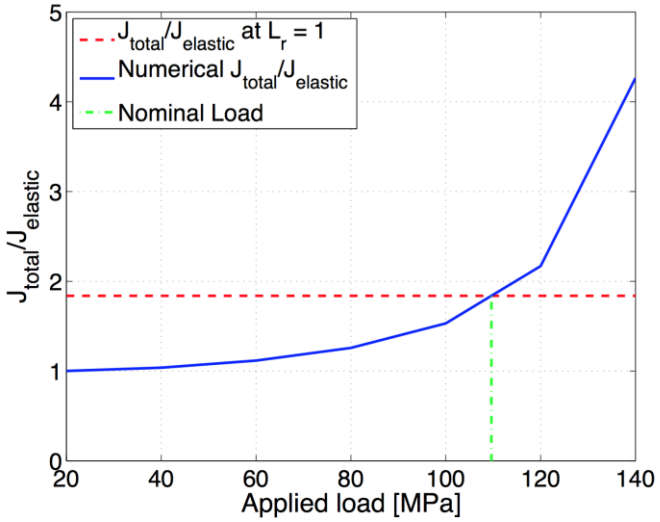

Figure 12: Identifying $\sigma_{nom}\,|_{L_r=1}$

With F calculated, the applied stress σ_a at each load increment may be converted into a reference stress by the relationship $\sigma_{ref} = F\sigma_a$. Finally, the plastic collapse ratio for each σ_a

can be calculated by $L_r = \frac{\sigma_{ref}}{S_y}$. The ordinate values of the MS-FAD curve are also calculated using the J-integral ratio. Specifically, K_R is given by: $K_r = \sqrt{\frac{J_{elast}}{J_{tot}}}$. The final step for generating a MS-FAD is to determine the maximum value of L_r. Typically, this is given by: $L_{r,max} = \frac{S_u}{S_y}$, where S_u is the tensile strength of the material. Plotting K_r against L_r and cutting off the curve at $L_{r,max}$ gives the MS-FAD, as shown in Figure 13.

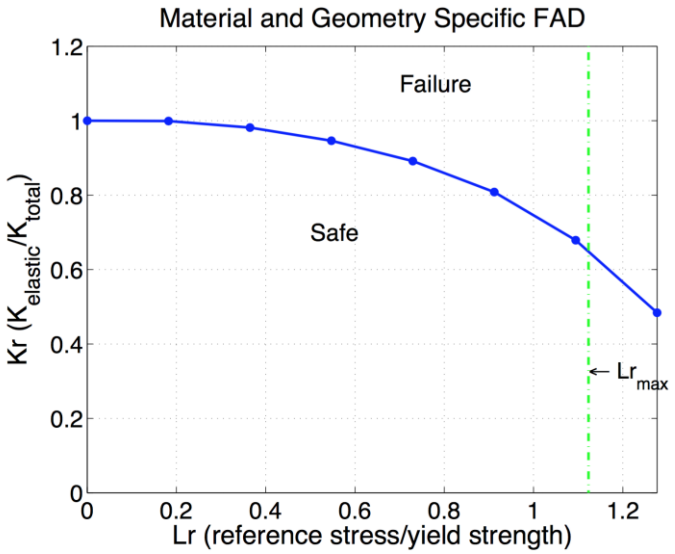

Figure 13: Material-specific FAD

As Fig. 14 shows, a crack was assumed to be initiated at the bending corner of the FW structure of a DEMO water-cooled blanket (Huang, et al., 2018), where the temperature is below 350 ˚C and the stresses are relatively high. The MS-FAD method requires computing the J-integral based on the elasto-plastic material model. For simplicity, the MS-FAD method was implemented on a 2D cross-section with two J-integral contours.

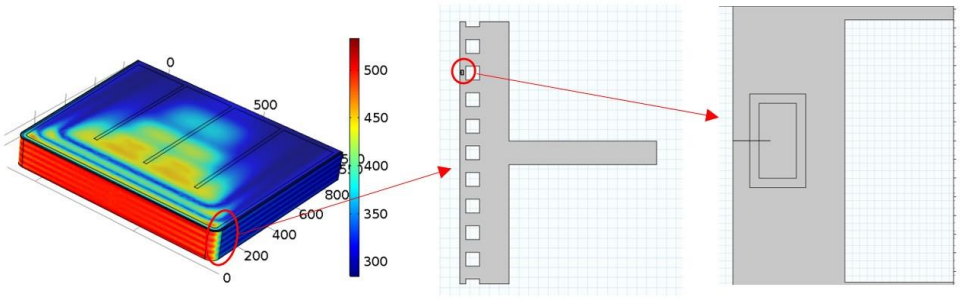

Figure 14: : Crack at FW corner with J-integral contours

For the reference stress calculation for the crack, both the elastic portion of the total elasto-plastic J-integral results and elasto-plastic J-integral were computed, based on the elastic material model and elasto-plastic stress-strain curve of Eurofer, respectively (Huang, et al., 2018). A parametric sweep was performed on the applied heat loading. The relative heat loading in the figures is defined as the ratio of applied The ratio $J_{tot}/J_{elastic}$ is plotted, and used to determine the values of the brittle fracture ratio K_r on the MS-FAD curve: $K_r = J_{elastic}/J_{tot}$. The MD-FAD curve can thus be generated specifically for Eurofer by plotting K_r versus L_r, as shown in Figure 15. The safety factor is computed for each value of the applied heat flux as the ratio of the *Kr* at the intersection between the load line and the FAD line to the value of *Kr* at the applied heat flux. It can be seen that the safety factor is around 1.16 at a surface heat flux of 0.8 MW/m2. This value corresponds to a fracture toughness of around 100 MPa$\sqrt{}$m at the operating temperatures, evaluated from the irradiation data at 3.5 dpa.

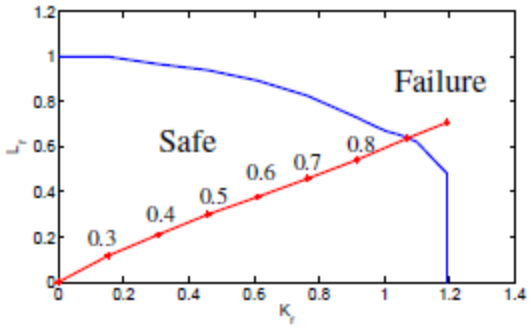

Figure 15: MS-FAD fracture analysis for the Eurofer 97 FW. The thermal load line is shown, where the surface heat flux is gradually increased (values are shown above the red line in unit of [MW/m2])

Crack propagation Simulations:

Fracture is a complicated process that depends strongly on factors such as loading conditions, geometry, and material properties. Cracks are seldom loaded in the traditional modes (opening, sliding, and twisting) separately, and generally have 3-dimensional character. Despite many efforts in the field of fracture mechanics, most realizations are two-dimensional, and threshold material properties (e.g. fracture toughness) are usually measured under plane strain conditions. Progress in fracture mechanics of truly 3D cracks of complex shapes has been slow, even though experimental observations strongly suggest that cracks generally possess 3D characters.

The FAD failure assessment discussed in the previous section is based on the assumption of a critical crack size in the FW or divertor structures. The critical size is determined from Non-Destructive Evaluation (NDE) procedures based on ultrasonic, dye penetration, or other methods. However, since the operation of DEMO is expected to be pulsed with variations in the stress and temperature fields, it is necessary to simulate actual crack growth under these operational conditions. Additionally, when cracks grow, practical calculations of the elastic field around propagating cracks can be a real challenge. These numerical difficulties stem from one fundamental fact: most current numerical techniques try to satisfy boundary conditions of the elastic field at the crack tip, although it is known to have an essential singularity. It is therefore desirable to have the ability to predict the behavior of 3-D cracks of arbitrary shapes under complex loading conditions in a manner that is not sensitive to the discretization details (i.e. mesh size) close to a propagating crack.

The more popular numerical method for simulations of slow crack growth is the eXtended Finite Element Method (XFEM) (Dolbow & Belytschko, 1999). While the method is relatively mesh-insensitive, it still requires elements to be small compared to the crack size, which is a potential issue when considering small-scale cracking(Dolbow & Belytschko, 1999). Some of the difficulties with the XFEM method are demonstrated in Figure 16 that shows the need to reduce the FEM mesh size to accommodate small cracks, and the care that must be taken for

nodal shape function enrichment when cracks traverse elements or reside entirely inside one element.

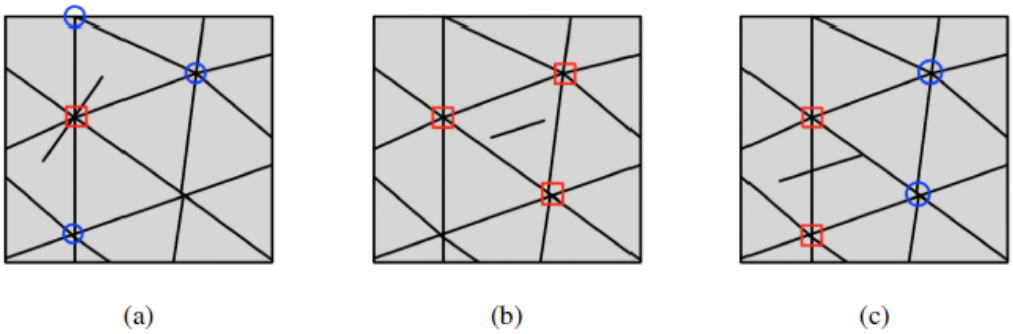

Figure 16: (a), (b), and (c) show cases in which cracks are on the same length scale as XFEM mesh elements.

An alternate method that can be used at this continuum level of life assessment is a dislocation-based crack modeling method: The Discrete Crack Mechanics method (DCM) (Takahashi, Ghoniem, & N.M., 2013) (Takahashi, Ghoniem, & N.M., 2013). In this approach, cracks are constructed using discrete Volterra dislocation loops. The methodology allows for the natural introduction of displacement discontinuities, thus avoiding numerically expensive techniques. The mesh-dependence in existing computational fracture modeling of propagating cracks is eliminated by utilizing a superposition technique. The elastic field of cracks in finite-bodies is separated into two parts: (1) the infinite-medium solution of discrete dislocations, and (2) a Finite Element Method (FEM) solution of a regular boundary correction problem to satisfy external boundary conditions. In the DCM method, a crack is fully represented by a dislocation array with a fixed outer loop that determines the position of the crack tip, plus additional concentric loops that are free to expand or contract. Once the equilibrium positions of the inner loops are found, the crack shape and stress field are completely determined. A variational formulation of the equation of motion governing the crack tip is developed for problems of quasi-static crack growth.

The DCM method was numerically verified for convergence and accuracy through several 2D and 3D crack problems with well-known solutions. The method was then applied to 3-D problems of unstable crack growth under load control, and to stable crack growth under displacement (rotation) control. In the latter case, a semicircular surface crack in a bent prismatic beam is shown to continuously change its shape as it propagates inward. Its mid-section advances slowly, while the side flanks of the crack grow at a faster rate towards the beam sides, unzipping its side surfaces to accommodate the imposed external rotation (Sheng, Ghoniem, Crosby, & Po, 2018).

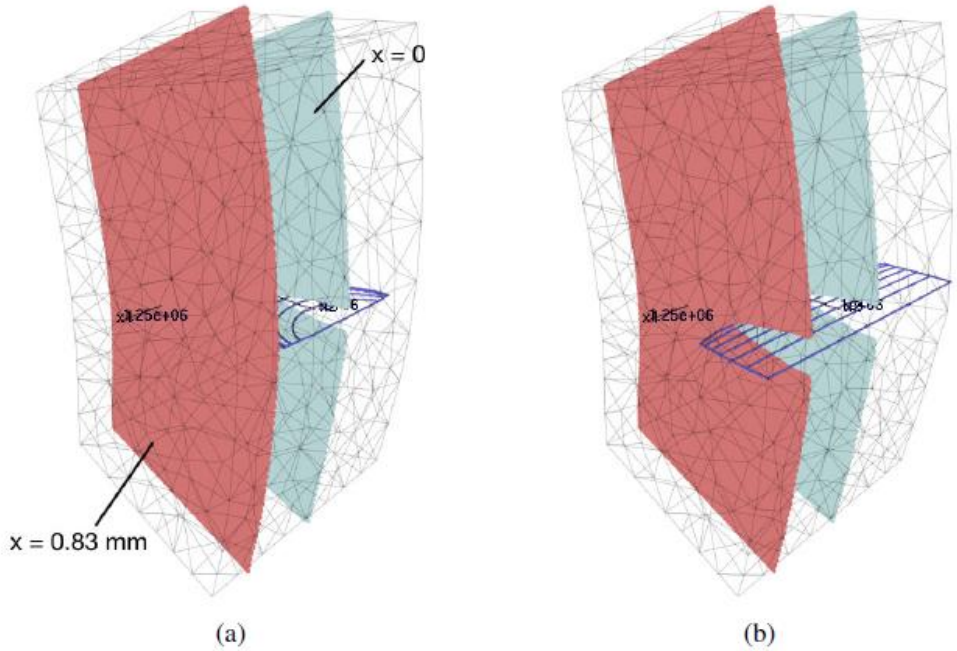

Figure 17: Cross-sections showing crack opening displacement X 100 for (a) initial crack state and (b) final crack state (Sheng, Ghoniem, Crosby, & Po, 2018).

If the edge crack continues to grow upon reaching the lateral faces of the beam, an "unzipping" of the beam occurs. This is modeled with the DCM method by confining the regions of the crack that intersect the lateral surfaces to move only along those surfaces. This unzipping is illustrated in Figure 17, which also shows the displacement magnified by 100 at two cross-sections of the beam (Sheng, Ghoniem, Crosby, & Po, 2018).

Evaluation of Low-Cycle Fatigue (LCF) life:

The intermittent operation of DEMO will be associated with the accumulation of plastic strain around notches, corners and other stress concentration locations in the FW/ Blanket structure and divertor elements. When the number of fatigue cycles is less than $\sim 10^3 - 10^4$ cycles, fatigue data on the standard S-N curve show very small changes in the fatigue strength. However, the material is usually deformed macroscopically in a plastic manner. In design practice, the analysis of low-cycle fatigue is usually done by describing the fatigue life as a function of the strain amplitude rather than the stress amplitude. The stress-strain changes significantly during cycling, with some materials exhibiting strain hardening while others exhibit strain softening. The computational challenge here is to perform fully elasto-plastic analysis on the FW/B or divertor structures and determine the equivalent (under multiaxial loading) strain amplitude components (both elastic and plastic) in the zones of the highest stress concentration.

In Figure 18, it is seen that experiments performed under strain control show the hysteresis stress-strain loops tend to stabilize after a few cycles. If a curve is drawn through the tips of these hysteresis loops, a cyclic stress-strain diagram is obtained, as shown in Figure 19.

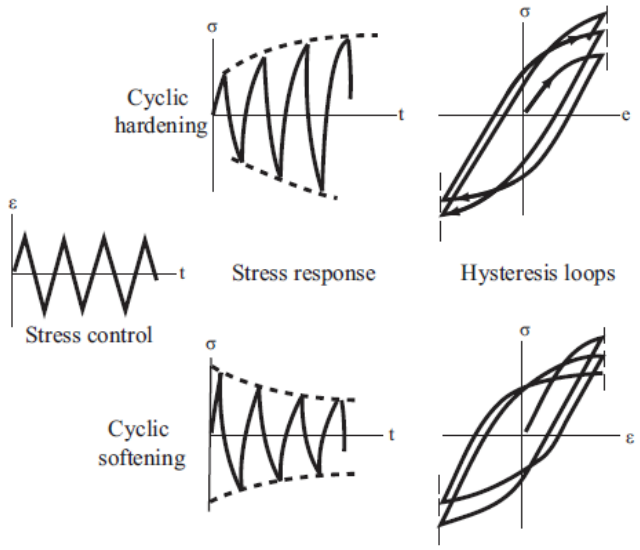

Figure 18: Illustration of cyclic strain hardening and strain softening phenomena under strain.

Experiments indicated that when the plastic component of the strain range ($\Delta\varepsilon_P$) is plotted against the number of cycles to failure on a log-log plot, the data exhibits a straight line with a slope of -0.5 to -0.7. However, low cycle fatigue data are represented by plotting the total strain amplitude ($\frac{\Delta\varepsilon}{2}$) against the number of reversals ($2N_F$) to failure. The cyclic strain amplitude is separated into an elastic component $\left(\frac{\Delta\varepsilon^e}{2}\right)$and a plastic component$\left(\frac{\Delta\varepsilon^P}{2}\right)$, and can be written in the form:

$$\frac{\Delta\varepsilon}{2} = \frac{\Delta\varepsilon^e}{2} + \frac{\Delta\varepsilon P}{2} = \frac{\Delta\sigma}{2E} + \left[\frac{\Delta\sigma}{2k}\right]^{1/n}$$

where k is the cyclic strength coefficient, and n is the cyclic strain hardening exponent. Both k and n are obtained from the cyclic stress-strain curve (see Figure 19). If the total cyclic strain data is represented as a function of the number of reversals ($2N_F$), on a log-log plot, the total curve can be shown to be the sum of two straight lines; one for the elastic strain, while the other is for the plastic strain amplitude. Thus, mathematically, the data can be represented as

$$\frac{\Delta\varepsilon}{2} = \frac{\sigma_f}{E}(2N_f)^b + \varepsilon_f(2N_f)^c$$

where the constants b and $\frac{\sigma_f}{E}$ are the slope and one-reversal intercept of the elastic curve. Also, the constants c and ε_f are the slope and one-reversal intercept of the plastic curve, as shown in Figure 19. Typical values of b are in the range -0.05 to -0.15 and c in the range -0.5 to -0.8. It is now clear that once we have the true stress strain data and the cyclic stress-strain curve, the curves for low cycle fatigue life prediction can be readily obtained. It is interesting to note that materials with high ductility will be superior for design applications in the low-cycle fatigue range (below the transition life). On the other hand, if the design requires performance in the high-cycle fatigue range, superior materials will be those which have higher fatigue strength.

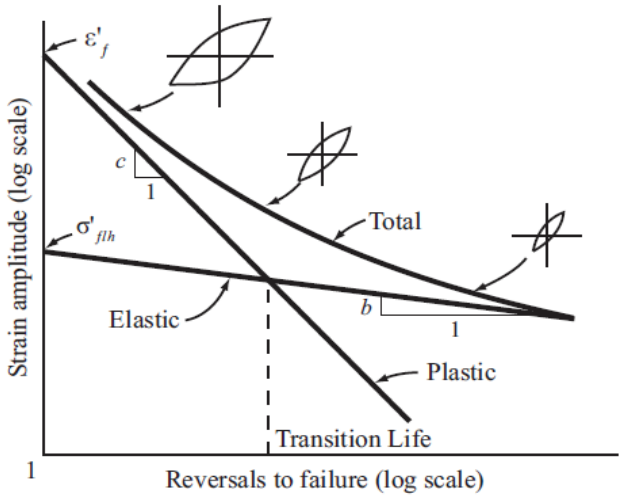

Figure 19: Schematic representation of elastic, plastic, and total strain amplitude versus fatigue life.

Temperature fluctuations can result in stress/strain cycles in mechanical components which are constrained from free expansion. It is therefore expected that the results of the analysis in this section would apply equally well to the case of thermally-induced stress cycles. Thus, thermal fatigue can be qualitatively similar to mechanical fatigue. However, the number of cycles to failure under thermal fatigue conditions can be shorter than the equivalent mechanical fatigue at the same average temperature. The reason appears to be related to several factors: (1) plastic strains tend to concentrate in the hottest regions because of the lower yield point at high temperatures; (2) material properties change due to thermal cycling.

Another important factor in determination of the effects of low-cycle fatigue is the influence of high energy neutron irradiation and helium production by 14 MeV neutrons on the strain-life correlations discussed above. While irradiated structures are known to strengthen under irradiation, they also lose ductility. The small amplitude stress fluctuations expected in the FW/B and divertor structures will result in high cycle fatigue, where fatigue damage is accumulated over tens of thousands to millions of cycles. As such, we expect that neutron irradiation will actually improve the high cycle fatigue life because of its effect on hardening and the increase in the yield strength. However, the situation will be the opposite as irradiation degrades the available ductility for a given number of plastic strain cycles in the low-cycle fatigue regime. Thus, the predicted lifetime will depend on whether the improvements in the high cycle

fatigue would be sufficienct to offset the negative effects of ductility loss when the strain amplitudes are high, for example, as a result of large temperature fluctuations induced by plasma disruptions.

6.7. Level-III: Microstructure-Based Analysis

- The "Multiscale method" for plasticity and fracture
- Example of "Microstructure-Based" Implementation
- How to couple the multiscale method with continuum elasto-viscoplasticity

7. Deployment Time-line

Full implementation of the Multiphysics-Multiscale design methodology is expected to take between 10 and 15 years. The speed of implementation is heavily dependent on available resources and accelerated multiscale modeling research on irradiated materials world-wide. Rather than being specific on the exact timeline for deployment of this design methodology, we specify elements of the program as "immediate", "near term" within the next decade, and "long term" for elements extending in the following decade. The programmatic elements are as follows:

- Enhanced Elastic Analysis (immediate).
- Elastoplastic Analysis (immediate).
- Continuum elasto-viscoplastic analysis (near term).
- Fracture Mechanics, J-Integral, plasticity effects – (near term).
- Probabilistic assessments (long term).
- Microstructure-Based Elasto-viscoplastic-damage modeling (long term).
- Combined Radiation-Thermomechanical Damage modeling to feed data into Microstructure-Based modeling (long term).

The proposed timeline is shown graphically in Figure 20, where the approximate duration for each area is indicated in years.

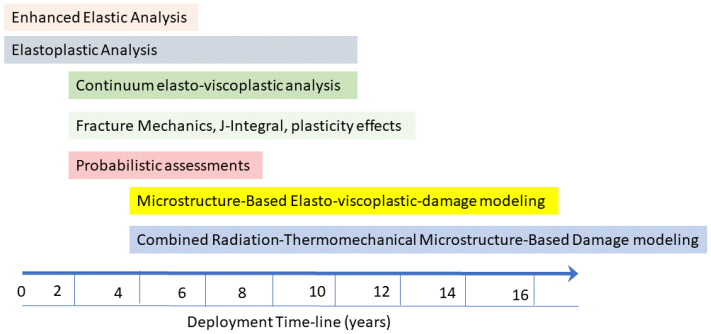

Figure 20: Approximate time-line for the development of DEMO design criteria that are based on microstructure information.

8. Conclusions and Recommendations

Assuring the structural integrity and reliability of the First Wall, Blanket, and Divertor structures of DEMO is of paramount importance. Without reliable, long-life components, the safety and economic viability of the entire power plant would be at jeopardy. To meet this critical goal, the mechanical design process must be established with the most advanced tools that are currently available. The successful design of DEMO will have to evolove from the current state of knowledge, verified by the operation of similar components in ITER and in other simulation facilities. The discriminating fact about DEMO is that it is one-of-a-kind, and there are no devices that have been built from which we can garner empirical knowledge. We will have to spring forward from what we presently know, and from the operational experience of ITER, to a satisfactory design process.

In other one-of-a-kind technological endeavors, such as most aerospace and demanding aircraft applications, there is a significant investment of resources dedicated to develope resilient materials in the face of harsh and partially unknown environments. For example, the development of turbine blade materials in modern jet engines has gone through several decades of continuous improvement through empiricism, and more recently, through a science-based approach. Turbine baldes have been developed first from nickel-based super-alloys, and as a result of more scientific understanding, single crystals were produced to control high-temperature creep properties. Next, special protection schemes were advanced to manufacture a stable top layer of Thermal Barrier Coatings (TBC) that allowed higher operational temperatures and better overall performance. Current efforts utilize advanced elastoplasticity and viscoplasticity models of the type described in this report to design turbine blades at higher performance levels. Future emphasis in this area is focused on the development of ceramic matrix composites that can allow even higher engine temperature and significant savings in the weight as a result of reduction or elimination of active cooling. The design of DEMO components must proceed in a similar fashion and embrace the

concepts of design-by-analysis rather that design-by-rules. The goal of this report is to furnish the background and necessary process to move forward and embrace a more methodical and quantitative method of design.

If we look closely at the current state of knowledge on the development of materials and components that could meet the stated goals of ITER, we are faced with two seemingly diverging approaches that must be reconciled. On the one hand, tremendous research efforts are being invested in the materials science aspects of radiation effects as they relate to the fusion environment, while component development, on the other hand, is based on approaches that do not consider much of this science base into the process. One has to wonder how such two approaches can be reconciled into a process that can have significant effects on both? The fusion materials scince field tends to emphasize the physics of defects as they are produced by neutrons or plasma ions. However, component design is based on elastic analysis augmented by empirical rules that have been slowly extrapolated from the early days of piping and pressure vessel design in the ASME code. The process described in this report is intended to reconcile the two approaches of research. The materials science approach will benefit because problem definition will not be arbitrary but will be linked to and end goal of assuring the structural integrity of ITER. On the other hand, the design approach will benefit from the significant data base on radiation effects and material properties. Microstructure-relevant information will be an integral part of the design process so that one can relate manufacturing, microstructure and properties in a meaningful way.

We outlined here a clear path towards achieving these goals. The approach is a top-down approach, where incremental advaces can be readily accommodated. The difficulty in the traditional hierarchical approach, starting from ab initio and progressing to Molecular Dynamics, Monte Carlo, Dislocation Dynamics and then the continuum is that it is simply too ambitious. The proposed top-down approach, however, is almost guarantted to function, and will get better as more knowledge accumulates from lower length scale studies. At the top level, Multiphysics modeling can be readily used with combined heat transfer, fluid mechanics and enhanced elastic structural mechanics. This step is at hand, and in fact, multiscale can be implemented at the continuum level. The process has been recently demonstrated in the design of the WCLL FW/B design of DEMO (Huang, et al., 2018) and (Huang Y. , 2018). The multiscale aspect is twofold, one that is essentially a multigrid method for elastic analysis, and the other is an elastic solution in the entire structure coupled with an elastoplastic solution in critical stress concentration zones. What lies in the future is the demonstration that continuum damage mechanics will contain microstructure information that can be validated through dedicated discrete simulations of defects using Dislocation Dynamics and Knietic Monte Carlo.

A timeline is proposed to achieve the physics-based design goal of DEMO. Currently, enhanced elastic analysis and Multiphysics are pursued, and may be expanded to calibrate

key aspects that dictate computational efficiency and depth of analysis. The inclusion of continuum elastoplastic analysis has also been demonstrated by several researchers and would continue to provide valuable insight into the critical phenomena worthy of more attention. Such analysis is also possible to validate with current experimental simulation facilities for high heat flux, for example, even though simultaneous 14 MeV neutron irradiation may be lacking. Within the next 2-4 years, the emphasis should shift on three elements of the proposed program: (1) Continuum elasto-viscoplastic analysis; (2) Fracture Mechanics, J-Integral and plasticity effects; and (3) Probabilistic assessments. These types of studies will furnish the foundations for the two most important aspects of the proposed program. These are: Microstructure-Based Elasto-viscoplastic-damage modeling; and (2) Combined Radiation-Thermomechanical Damage modeling to feed data into Microstructure-Based modeling. It is suggested that preliminary research would continue into these two aspects, and a full-fledged program develops in 4 years' time, possibly continuing for a decade before full fruition into a complete design process for DEMO components.

9. Bibliography

Ainsworth, R. (1993). The use of a failure assessment diagram for initiation and propagation of defects at high temperatures. *Fatigue & Fracture of Engineering Materials & Structures, 16*(10), 1091-1108.

Aktaa, J., Kecskes, S., & Cismondi, F. (2012). Naon-linear Analysis of HCPB Test Blanket Module. *Fusion Engineering & Design, 87*(7-8), 1085-1090.

Bloom, E. E. (2007). Critical questions in materials science and engineering for successful development of fusion power. *Journal of Nuclear Materials, 367-370*, 1-10.

Boccaccini, L.V., & al., e. (2016). Objectives and Status of EUROfusion DEMO blanket studies. *Fusion Engineering & Design, 109-111*, 1199-1206.

Bree, J. (1967). Elastic-plastic behaviour of thin tubes subjected to internal pressure and intermittent high-heat fluxes with application to fast-nuclear-reactor fuel elements. *Journal of Strain Analysis*, 226-238.

Budden, P., & Ainsworth, R. (2012). The shape of a strain-based failure assessment diagram. *International Journal of Pressure Vessels and Piping, 89*, 59–66.

Conle, F., & Chu, C. (1997). Fatigue analysis and local stress-strain approach in complex vehicular structures. *International Journal of Fatigue, 19 (93)*, 317-323.

Corwin, W., & al., e. (2005). Updated generation IV reactor integrated materials program plan, Revision 2. Oak Ridge: ORNL/TM-2003/244/R2.

Dolbow, J., & Belytschko, T. (1999). A finite element method for crack growth without remeshing. *International journal for Numerical Methods in Engineering, 46*(1), 131-150.

Federici, G., Kemp, R., Ward, D., Bachmann, C., Franke, T., Gonzalez, S., . . . Morlock, C. (2014). Overview of the EU DEMO design and R&D activities. *Fusion Engineering & Design, 89(7)*, 882-889.

Huang, Y. (2018). *Multiscale Modeling of Dislocation-Based Crystal Plasticity within a Multiphysics Framework.* Los Angeles: University of California, Los Angeles (UCLA).

Huang, Y., Cismondi, F., Diegele, E., Federici, G., Del Nevo, A., Moro, F., & Ghoniem, N. (2018). Thermostructural Design of the European DEMO Water-cooled Blanket with a Multiscale-Multiphysics Framework. *Fusion Engineering & Design*, In Press.

Huckbusch. (2013). *Multigrid methods and applications.* Springer Scince and Business Media.

ITER Organization. (1998). *ITER structral design criteria for in-vessel components (ISDC).* ITER IDoMS S74MA1 97-12-12 RO.2, Appendix A IDoMS G74MA2 98-06-26.

MacLennan, I., & Hancock, J. (1995). Constraint-Based Failure Assessment Diagrams. *Proceedings of the Royal Society of London, A 451*, 757-777.

Majumdar, S., & Smith, P. (1997). *Proceedings of the 4th International Symposium on Fusion Nuclear Technology (ISFNT-4).* Tokyo.

Neuber, H. (1961). Theory of Stress Concentration for shear strained prismatical bodies with arbitrary non-linear stress-strain law. *Journal of Applied Mechanics, 28*, 544-550.

Park, K., & Felippa, A. (2000). A variational principle for the formulation of partitioned structural systems. *International Journal of Numerical Methods in Engineering, 47*(1-3), 395-418.

Romanelli, F. (2012). *A roadmap to the realization of fusion energy.* EFDA.

Sheng, A., Ghoniem, N., Crosby, T., & Po, G. (2018). A mesh-independent method for three-dimensional crack growth in finite geometry. *International Journal for Numerical Methods in Engineering*, Under Review.

Takahashi, A., Ghoniem, & N.M. (2013). Fracture mechanics of propagating 3-d fatigue cracks with parametric dislocations. *Philosophical Magazine, 93*(20), 2662-2679.

Appendix A: ISDC-IVC

To understand design criteria, we briefly discuss here the main definitions in the ITER design code:

1. *Primary stress:* primary stress is defined as that portion of the total stress which is required to satisfy equilibrium with the applied loading and which does not diminish after small scale permanent deformation.
2. *Secondary stress:* secondary stress is that portion of the total stress (minus peak stresses, as defined below), which can be relaxed as a result of small scale permanent deformation. The basic characteristic of a secondary stress is that it is self-limiting.
3. *Total stress (strain):* total stress σ_{ij} (strain ε_{ij}) is the stress (strain) under the effect of all the loadings to which the component is subjected.
4. *Membrane stress (strain):* membrane stress (or strain) tensor is the tensor whose components $(\sigma_{ij})_m$ [$(\varepsilon_{ij})_m$] are equal to the mean value of stresses σ_{ij} (ε_{ij}) through the thickness.
5. Bending stress (strain): the bending stress (strain) tensor is that tensor whose components $(\sigma_{ij})_b$ [$(\varepsilon_{ij})_b$] vary linearly through the thickness and which, when integrated through the thickness result in equilibrium with the section moment.
6. *Peak stress:* Peak stress is the increment of stress which is additive to the membrane-plus-bending stresses by reason of local discontinuities or local thermal stresses including the effects, if any, of stress concentrations.
7. *Stress intensity:* the stress intensity, $\bar{\sigma}$, at any given point is a scalar derived from the stress tensor, σ , at that point, using the maximum shear or Tresca criterion.
8. *Effective stress:* the effective stress used for creep calculation is based on von-Mises effective stress.
9. *Stress intensity range:* it is the maximum of the stress intensities of the tensor differences between the stress tensors $\sigma(t)$ and $\sigma(t$ for every pair of times t and t' within a cycle.
10. *Allowable primary membrane stress intensity (S_m)*: S_m is a temperature (T) and fluence (Φt) dependent allowable stress intensity defined as the least of the quantities:

$$S_m = Min\left[\frac{1}{3}S_{u,min}(RT,0),\frac{1}{3}S_{u,min}(T,0),\right.$$
$$\frac{1}{3}S_{u,min}(T,\Phi t),\frac{2}{3}S_{y,min}(RT,0),$$
$$\left.\frac{2}{3}S_{y,min}(T,0),\frac{2}{3}S_{y,min}(T,\Phi t)\right] \qquad (90)$$

where $S_{y,min}$ and $S_{u,min}$ are the minimum yield and ultimate tensile strengths, respectively, and RT is room temperature.

11. *Uniform elongation* (ε_u): ε_u is defined as the plastic component of the engineering strain at the time when necking begins in a uniaxial tensile test.
12. *True strain at rupture* (ε_{tr}): ε_{tr} is defined as : $\ln\frac{100}{100-RA\%}$, where %RA is the reduction in area (%) as determined in a uniaxial tension test at a given temperature, strain rate, and fluence.
13. *Elastic follow-up factor (r):* the r-factor provides a simplified inelastic analysis approach by which the peak inelastic strain and stress in a structure can be estimated from elastic analysis results. An r value equal to 4 is used in ISDC as a conservative estimate for many structures made of ductile alloys with adequate strain-hardening capability.
14. *Allowable primary plus secondary membrane stress intensity (S_e)*: S_e is a temperature (T) and fluence (Φt) dependent allowable stress intensity for a material with severe loss of uniform elongation due to irradiation and is defined as follows:

$$S_e = \begin{cases} \frac{1}{3}S_{u,min}(T,\Phi t) + \frac{E\alpha_1}{r_1}(\varepsilon_u(T,\Phi t) - 0.02) & if\ \varepsilon_u > 2\% \\ \frac{1}{3}S_u, min(T,\Phi t) & if\ \varepsilon_u < 2\% \end{cases} \quad (91)$$

where E is Young's modulus, $\alpha_1 = 0.5$, and $r_1 = \infty$ for $\varepsilon_u < 2\%$, and $r_1 = 4$ for $\varepsilon_u > 2\%$

15. *Allowable total stress intensity (S_d)*: S_d is a temperature (T), fluence (Φt), and r-factor dependent allowable stress intensity for total primary plus secondary stress in radiation embrittled materials, and is defined as follows:

$$S_d = \frac{2}{3}\left(S_{u,min}(T,\Phi t) + \frac{E\varepsilon_{tr}(T,\Phi t)}{r \times TF} \right) \quad (92)$$

where TF = triaxiality factor to account for the effect of hydrostatic stress on ductility: $TF = (\sigma_1 + \sigma_2 + \sigma_3)/\sigma_e$. and r = elastic follow-up factor whose value is r_2 in zones of stress concentration (i.e., peak stress due to stress concentration is included), and r_3 away from zones of stress concentration. r_2 = Max {K_T & 4} where K_T is the elastic stress concentration factor and $r_3 = r_1$.

16. *Time-dependent allowable primary stress intensity (S_t):* S_t is a time and temperature-dependent allowable primary stress intensity defined as the least of the following: (1) two thirds of the minimum stress corresponding to average creep rupture time t at temperature T, (2) 80% of the minimum stress corresponding to time t and temperature T for onset of tertiary creep, and (3) minimum stress to cause a creep strain of min[1%, ε_C /5] in time t and temperature T, where ε_C is the minimum creep ductility.

The design rules are divided into a high temperature section and a low temperature section, depending on whether thermal creep effects are or are not important. The low temperature rules are always applicable. To determine whether the high temperature rules are also to be

applied, the following negligible creep test should be used. Thermal creep is negligible over the total design lifetime of a component if the following summation limit is satisfied:

$$\sum_{i=1}^{N}\left(\frac{t_i}{t_{ci}}\right)\le 1 \tag{93}$$

where the total lifetime is divided into N intervals of time; for each interval i, of duration t_i, the maximum allowable time at temperature is denoted by t_{ci}. The negligible thermal creep time t_{ci} at a temperature T_i is calculated as the time required to accumulate a thermal creep strain of 0.05% in a uniaxial creep specimen subjected to a constant stress of 1.5 $S_m(T_i)$. If the inequality in Equation 93 is satisfied, then only low temperature design rules need be applied. The following is a list of the design rules that must be met for components made of any structural material, and that we will apply to specific F/M alloys.

- Low-Temperature Design Rules:
  (a) *Necking and plastic instability limit*: To prevent failure by necking and plastic instability, the following limits must be satisfied at all times:

  $$\overline{P_m}\le S_m;\quad \overline{P_L+P_B}\le KS_m(T_m,\Phi t_m). \tag{94}$$

  where P_m is general primary membrane stress, P_L is local primary membrane stress, P_b is primary bending stress, K is bending shape factor (= 1.5 for solid rectangular section), and S_m is evaluated at the thickness-averaged temperature (T_m) and fluence $(\Phi t)_m$

  (b) *Plastic flow localization limit*: To prevent cracking due to plastic flow localization (in a material with significant loss of uniform elongation due to irradiation), the following limit must be satisfied at all times during the life of the component:

  $$\overline{P_L+Q_L}\le S_e(T_m,\Phi t_m). \tag{95}$$

  (c) *Ductility exhaustion limit*: To prevent local fracture due to exhaustion of ductility (due to embrittlement), the following limits must be satisfied at all times during the life of the component: The total stress, including peak stress, is limited by

  $$\overline{P_L+P_b+Q+F}\le S_d(T,\Phi t,r_2) \tag{96}$$

  where F is peak stress (e.g., due to stress concentration), and the total stress, excluding peak stress, is limited by

  $$\overline{P_L+P_b+Q}\le S_d(T,\Phi t,r_3) \tag{97}$$

  (d) *Brittle fracture limit*: To prevent brittle fracture initiating from severe flaws or notches, the maximum mode I stress intensity factor, K_I, due to all primary and secondary loadings, including peak (P_L+P_b+Q+F), must be limited by the following:

  $$K_I\le K_C(T_m,\Phi t) \tag{98}$$

where K_C is the linear-elastic fracture toughness evaluated at the thickness-averaged temperature and fluence. The stress intensity factor K_I has to be determined from the analysis of a postulated surface flaw of depth a_0, length $4a_0$, where $a_0 = max[4a_u, h/4]$, a_u = largest undetectable crack length, and h = section thickness. If the full section under consideration (without the flaw) experiences plasticity, a suitable non-linear fracture parameter (e.g., J-integral) should be used instead of K.

(e) *Ratcheting limit*: To prevent ratcheting due to cyclic loading, either of the following two limits should be satisfied at all times:

i. 3 S_m limit: $\overline{(P_L + P_b)}_{max} + \Delta[\overline{P} + \overline{Q}]_{max} \le 3S_m(T_m, \Phi t_m)$

where Δ denotes the range of primary (P) and secondary (Q) stress due to cyclic loading.

ii. Bree-diagram limit:

$$Y \le \begin{cases} \dfrac{1}{X} & for\ 0 \le X \le 0.5 \\ 4(1-X) & for\ 0.5 < X \le 1 \end{cases} \qquad (99)$$

where $X = \dfrac{\overline{P_m}}{S_y}$ or $X = \dfrac{\overline{P_L + \dfrac{P_b}{K}}}{S_y}$ and $Y = \dfrac{\Delta[\overline{P} + \overline{Q}]}{S_y}$

and the yield stress S_y is evaluated at the average of the thickness-averaged temperatures at the cold and hot ends of the cycle.

(e) *Fatigue limit*: To prevent the initiation of a fatigue crack due to cyclic loading, the fatigue usage fraction V at the end of life must satisfy the following limit:

$$V = \sum_{j=1}^{J} \frac{n_j}{N_j(\overline{\Delta\varepsilon_j})} < 1 \qquad (100)$$

where the lifetime is divided into J type of cycles. For each cycle type j, characterized by n_j cycles at an equivalent strain range $\overline{\Delta\varepsilon_j}$ and average temperature T_j during the cycle, N_j is the allowable cycles. If $\overline{\Delta\varepsilon_j}$ is calculated elastically, it should be corrected for possible plasticity effects (e.g., by Neuber's rule for notches).

- High-Temperature Design Rules:

(a) *Creep damage limit*: To guard against creep damage, the following limits must be satisfied:

$$\overline{P_m} \le S_t(T_m, t)$$
$$\overline{P_L + P_b/K_t} \le S_t(T_m, t) \qquad (101)$$

where t is the design lifetime, and $K_t = (K+1)/2$. If the lifetime involves variable stress and temperature history, these equations should be replaced by limits on usage fraction sums.

(b) *Creep-ratcheting limit*: If the negligible creep test is not satisfied, then in addition to satisfying the low temperature ratcheting limit based on Bree diagram, the high temperature ratcheting limit should be satisfied by first calculating an effective core stress σ_c for creep calculations as follows:

$$\sigma_c = ZS_{yL} \tag{102}$$

where S_{yL} is the S_y value at the low temperature extreme of the cycle and Z is a creep stress parameter defined in terms of X and Y, as follows:

$$Z = \begin{cases} X & for\ X+Y \le 1 \\ Y+1-2\sqrt{(1-X)Y} & for\ 1-X \le Y < \dfrac{1}{(1-X)} \\ XY & for\ Y > \dfrac{1}{1-X} \end{cases} \tag{103}$$

The total creep strain accumulated during the lifetime due to a stress 1.25 σ_c should be less than min[1%, $\varepsilon_C/5$] where ε_C is the minimum creep ductility during the cycle. If the lifetime involves more than one types of cycles of stress and temperature, the criterion is satisfied by the use of usage fraction sums.

(c) *Creep-fatigue limit*: If the negligible creep test is not satisfied, then creep damage (W) has to be added to the fatigue damage (V) evaluated as:

$$V + W < 1 \tag{104}$$

where W is the creep damage obtained by first dividing the lifetime into K intervals. Each interval k of duration t_k is characterized by a maximum temperature T_k, a maximum effective stress $\sigma_{e,k}$. The following sum defines the creep damage W:

$$W = \sum_{k=1}^{K} \frac{\Delta t_k}{t_{R,k}} \tag{105}$$

where $t_{R,k}$ is the minimum time to creep rupture at temperature T_k and stress 1.25 $\sigma_{c,k}$.

A summary of the design procedure is shown in the figure below.

Analysis Flow Chart for Low-Temperature SDC-IC Design Rules for Given Operating Conditions

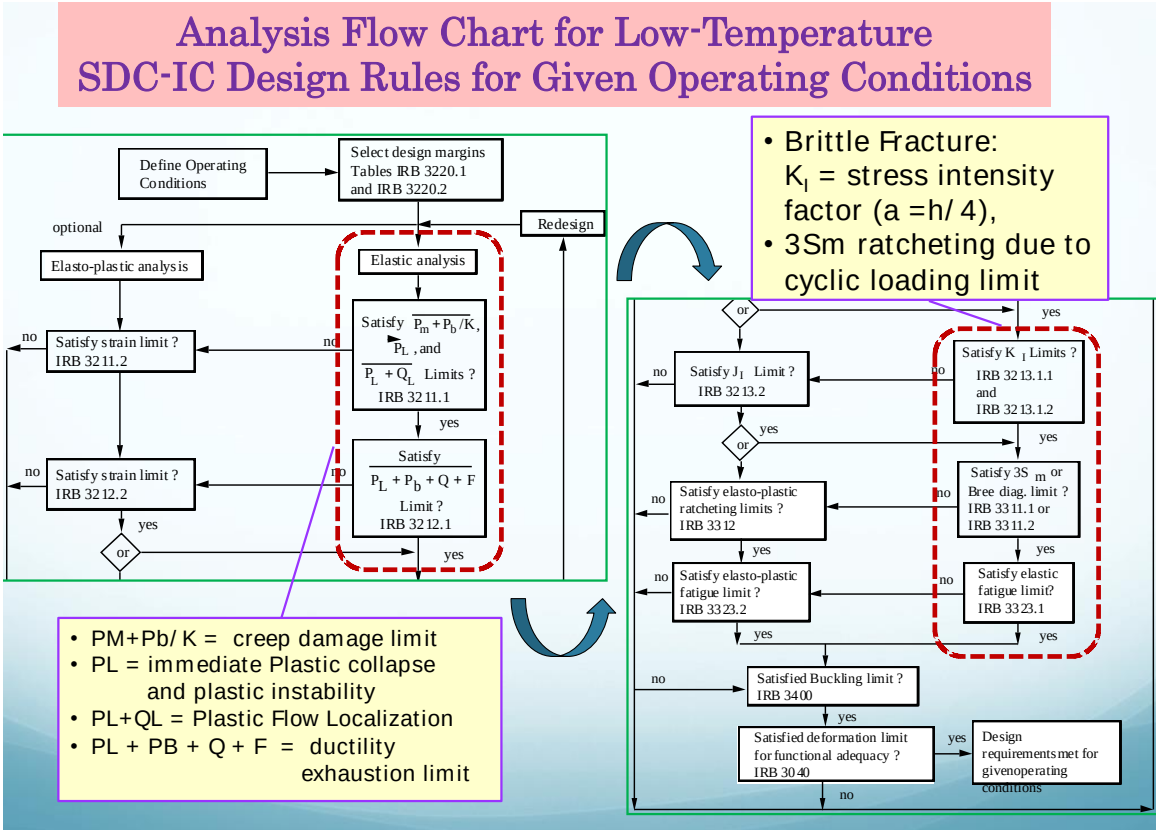

Appendix B: Codes and Standards

Standard: A standard consists of technical definitions and guidelines that functions as instructions for designers/manufacturers and operators/users of equipment. Standards can run from a few pages to a few hundred pages and are written by professionals who serve on the committees. Standards are considered voluntary because they are guidelines and not enforceable by law.
Code: A code is a standard that has been adopted by one or more governmental bodies and is enforceable by law.

As previously highlighted, if possible a SIC-1 component needs to follow Nuclear Codes during the licensing process. An alternative to a Nuclear Code should only be used if an appropriate design code does not exist. Currently, the two major Nuclear Codes come from ASME and AFCEN, neither of which fulfils the needs of DEMO. This is the primary reason as to why the need for a DEMO design criteria was identified. However, the ideal solution would be to integrate the development of the DDC into both AFCEN and ASME Code suites. This integration needs to be fully completed by 2027 so that these Codes could be used during the engineering design phase and beyond. From an idealistic standpoint, the creation of an International Fusion Code (ISO) would be highly beneficial and should be explored as an option.

Appendix C: Categories of Structures, Systems, and Components

The WPSAE team has proposed the following categories for SSC (Structures, Systems and Component):

An SSC is classified as **SIC-1** if:

- its failure could lead to an event with consequences exceeding one-tenth of the limits set out in section 5.2.1 of the DEMO PSRD [3] or
- it is needed to prevent, detect or mitigate an accident from resulting in consequences exceeding the limits set out in section 5.2.1 of the DEMO PSRD [3] or
- it is needed to bring and maintain the plant into a safe state.

An SSC is classified as **SIC-2** if:

- its failure could lead to an event with consequences exceeding a dose of 100 μSv to the most exposed individual member of the public, or
- it is needed to prevent, detect or mitigate an incident or accident, although not required to reach a safe state, or
- it is needed to ensure adequate shielding from radiation during normal operation.

An SSC is classified as **SIC-3** if:

- its failure could lead to an event with consequences exceeding a dose of 10 μSv to the most exposed individual member of the public, or
- although not needed to prevent, detect or mitigate an incident or accident, it helps to further reduce the consequences of such an event.

All other components are classed as Non-SIC.

The following table summarizes the different requirements for each of the SIC classifications:

Safety classified SSCs	SIC-1	SIC-2	SIC-3
Single failure criterion/Separation [2]	Yes	Yes or No	No
Mechanical classification	Nuclear Standards, DEMO specification	Standards, DEMO specification	Standards, DEMO specification
Safety class power supply	Yes	Yes	Yes in general
I&C 61226	Cat A	Cat B	Cat C
Periodic tests	Yes	Yes	Normally yes (case by case)

Quality Class	QC1	QC2	QC3
Environmental qualification	Yes	Yes (by analysis normally)	Yes or No
Design resistant to design basis earthquake	SC1	SC1	SC2
Seismic qualification	S and F	S normally. F on a case by case basis	S

From the table, it is suggested that SIC-1 components should utilise established Nuclear C&S. However elsewhere in the document it also highlights that "Where an appropriate design code does not exist, an agreed surrogate developed specifically for DEMO may be used." From both statements, for SIC-1 components we should be working towards using established Nuclear C&S.

For SIC-2 and SIC-3 components the need to use Nuclear C&S is less important. As such alternative standards could be readily used if deemed necessary.

Currently it is envisaged that both the DEMO Divertor and Blankets are to be classed as SIC components. However, the exact class of SIC component has yet to be defined, and is highly dependent on design solution chosen, for example the amount of tritiated water retained within the BB shall directly affect the safety classifications.

In order to progress the rest of this report it shall be assumed that both the DIV and BB systems shall be SIC-1.